

DOI: https://doi.org/10.30898/1684-1719.2025.10.6

# COMPARISON AND CORRELATIONS OF SEASONAL-MEAN STATISTICAL PARAMETERS OF STRATOSPHERIC OZONE AND TEMPERATURE BY DATA OF GROUND-BASED RADIOMETRIC AND SATELLITE MEASUREMENTS IN 1996-2017

K.P. Gaikovich <sup>1</sup>, S.B. Rozanov <sup>2,3</sup>

Institute for physics of microstructures RAS,
 603950, GSP-105, Nizhny Novgorod, Russia
 P.N. Lebedev Physical Institute RAS,
 119991, GSP-1, Russia, Moscow
 Russian Metrological Institute of Technical Physics and Radio Engineering,
 141570, Russia, Mendeleevo, Moscow region

The paper was received July 14, 2025.

**Abstract.** The results of a statistical analysis and comparison of the seasonal-mean altitude profiles of ozone content in the stratosphere and lower mesosphere above Moscow, obtained from ground-based microwave radiometric measurements, and the corresponding temperature profiles from satellite data are presented. The analysis included ensembles of data for the autumn, winter, and spring seasons of the 1996-2006 and 2007-2017 decades, which coincided with the 23rd and 24th cycles of solar activity. Based on these data, the seasonal-mean altitude profiles of parameters and their variances, the joint ozone-temperature correlation and covariance functions, the inter-altitude correlation and covariance functions, as well as the frequency spectra of covariances were obtained. When comparing these statistical parameters over two decades, statistically significant correlations and trends were found. In particular, during the winter season of the 2007-2017 decade, when solar activity was reduced,

there was a significant decrease in seasonal-mean temperature profiles over a wide range of heights around the maximum of the ozone layer, up to -8.4 K at an altitude of 37 km. The result is particularly interesting because this decrease in the average winter temperature in the decade with reduced solar activity correlates with the most significant (up to 28 % at 38-39 km) decrease in the average winter variations in the ozone profile above 29 km, as well as with the decrease in its average decadal-mean variations, which we found earlier. For the first time in studies of the ozonosphere, seasonal-mean inter-altitude joint ozone-temperature correlation and covariance functions were applied and obtained for the decades 1996-2006 and 2007-2017. In particular, the areas of the greatest correlation of ozone with temperature, which are observed for temperatures at altitudes below 35 km, and the areas of the greatest anticorrelation, which are above this altitude, were identified.

**Key words:** remote sensing, microwave radiometry, ozone and temperature altitude profiles, stratosphere, statistical analysis.

**Financing:** This study has been supported by the Ministry of Science and Education of Russian Federation, program FFUF-2024-0019.

Corresponding author: Gaikovich Konstantin Pavlovich, gaikovich@mail.ru

## Introduction

The paper is an extended publication of the statistical analysis of the seasonal average statistical parameters of ozone content and temperature in the stratosphere and lower mesosphere above Moscow, which was partially presented in [1], and continues our research [2,3] related to the statistical analysis of ensembles of altitude profiles of ozone content formed from ground-based microwave radiometric measurements at the P.N. Lebedev Physical Institute of the Russian Academy of Sciences (LPI) from 1996 to 2017. In order to study ozone-temperature relationships, ensembles of corresponding altitude temperature profiles from available databases are included in the analysis in this article.

Currently, most of the information about the global distribution of ozone and temperature in the stratosphere and mesosphere is obtained from satellite

measurements [4]. However, the large scale of horizontal averaging, as well as variations in observation time and satellite trajectory, limit the accuracy of measurements, and the relatively short period of satellite programs limits the possibilities for long-term observations. In this regard, ground-based remote sensing of ozone becomes important, conducted in the same location and using the same method. This allows obtaining long-term series of homogeneous data with significantly better horizontal resolution. Such long-term series of high-altitude ozone content profiles were obtained as a result of radiometric measurements of the spectrum of microwave thermal radiation of the atmosphere at the frequencies of the rotational line of ozone centered at 142.175 GHz at the LPI in Moscow (55.70° N, 37.57° E) since January 1996 to May 2017) [2] and at the University of Bern (46.95°N, 7.44°E) from January 1997 to January 2015) [5].

The data obtained at LPI are of particular interest not only because of their duration, but also because they begin almost coinciding with the beginning of the ozone layer recovery [4], and the measurement period almost exactly coincides with the 23rd and 24th cycles of solar activity. The geographical location of Moscow in the zone of strong variations in stratospheric ozone associated with planetary waves and the transport of various air masses, including the arrival of ozone-poor air in the polar stratospheric vortex during the cold months, allows us to study both these processes and related trends in stratospheric ozone.

In previous papers [2,3], a statistical analysis of the ozone layer observation data in 1996-2017 was presented. This analysis is interesting because the 23rd and 24th solar cycles differed significantly in their activity. The dataset was divided into two 11-year ensembles: 1996-2006 and 2007-2017. To increase the statistical significance of the results, the monthly-mean profiles of the relative ozone content for each analyzed month (September to May) were averaged over 11 years of each decade. To estimate the overall changes between decades, the decadal-mean parameters were determined by averaging the average monthly profiles over all months of the analysis.

The most unexpected and inexplicable result of the statistical analysis was the detection of a sharp decrease in the variability (standard deviations) in the ozone profile

above 30 km in 2007-2017 compared to 1996-2006 [2,3]. As the main factors that could lead to such a significant decrease, we considered the different nature of the large-scale stratosphere dynamics of the Northern Hemisphere in the periods (decades) under consideration, as well as a strong drop in solar activity in the 24th cycle of 2007-2017. compared with the 23rd cycle of 1996-2006, shown in Fig.1 [2,3].

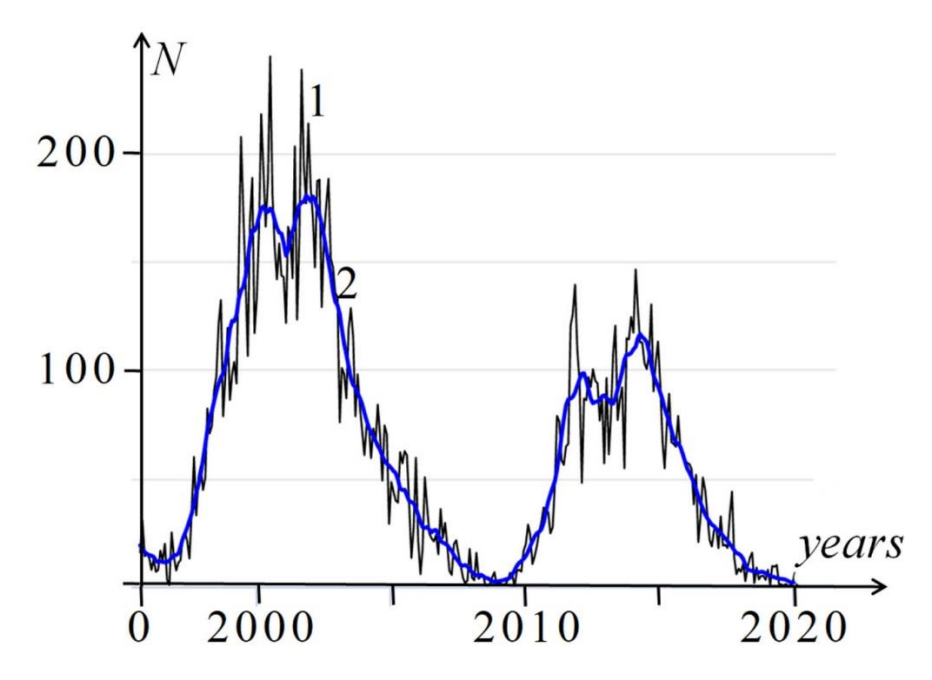


Fig.1. The 23rd and 24th cycles of solar activity: 1 – the average monthly number of sunspots; 2 – smoothed curve.

As can be seen in Fig. 1, solar activity in the 24th cycle was almost twice less than in the 23rd.

As is known, the content and dynamics of ozone distribution depend on the balance of rates of its photochemical formation, depending on solar radiation, losses in destructive processes involving compounds of hydrogen (H, OH, HO<sub>2</sub>), nitrogen (N, NO, NO<sub>2</sub>) and chlorine (Cl, ClO), as well as on large-scale ozone transport by air [4,6,7]. Dynamic processes also affect the temperature distribution, and an increase in temperature accelerates ozone depletion reactions [7]. According to modeling [8], the response of ozone in the upper stratosphere to temperature changes will increase as the chlorine content decreases. These processes lead to a negative correlation between ozone concentration and temperature in the upper stratosphere.

There are also experimental studies on the role of temperature and solar activity in the formation of high-altitude ozone distribution in various geographical areas. The

paper [5] presents the results of multiparametric regression analysis on fluctuations in average monthly ozone profiles during approximately 1.5 solar cycles, taking into account annual, semiannual and quasi-biannual fluctuations, El Nino Southern Oscillation and solar cycle (based on normalized time series of solar radio flux at wavelength 10.7 cm). A strong peak amplitude of approximately 5 % was observed for the component associated with solar cycle in the lower stratosphere.

Based on satellite measurements of ozone levels in the middle layers of the atmosphere, several scientific groups have investigated correlations between ozone, temperature, and solar activity. In [9], it was found that the seasonal-mean variations in ozone and temperature measured by the SABER instrument on board the TIMED satellite in the period from 2002 to 2005 in the latitude range 48N to 48S and at altitudes 20 to 100 km positively correlated approximately below 30 km and above 80 km, and were negatively correlated approximately between 30 and 80 km. Later, this group presented data on 10-year trends in ozone and temperature and their correlation over a longer period from 2002 to 2012 [10], as well as on the responses of ozone and temperature to fluctuations in solar activity from 2002 to 2014 [11]. They found that in the middle stratosphere and upper mesosphere, the ozone response to the solar cycle was relatively strong [12].

The analysis performed in [13] for the period 1979-2020 revealed a correlation between temperature in the lower stratosphere and total ozone content in the atmospheric column. This article noted that variations in the ozone content in the upper troposphere and lower stratosphere can influence the temperature in the middle and upper stratosphere through ascending long-wavelength radiation. Additionally, [8] found a correlation between ozone content and temperature in lower layers of the tropical stratosphere.

In [14], the frequency dependence of the correlation level between ozone and temperature over time periods from 2 days to 5 years was studied using data obtained from the Microwave Limb Sounder (MLS) instrument aboard the Aura satellite in 2004-2021, and for these periods the corresponding altitude areas of correlation and anticorrelation between ozone and temperature were determined.

The above results of the discovered correlations between ozone and temperature and the correlations of ozone content with solar activity, stimulated us to continue our research by incorporating temperature into the analysis of statistical parameters in order to investigate the joint ozone-temperature correlation and covariance functions, and to compare the statistical parameters of ozone and temperature obtained over two decades based on the same ensembles of ozone profiles obtained at LPI and ensembles of the corresponding temperature profiles from the available databases.

Considering that the main specifics related to the differences in the two decades relate to the winter months, unlike our paper [2], which shows the monthly-mean and decadal-mean statistical parameters of ozone, in this paper we present a comparison of the seasonal-mean (averaged over the monthly-mean profiles of each of the seasons) parameters for 1996-2006 and 2007-2017 to identify the specifics and differences of the winter season from the transitional autumn and spring seasons with greater statistical significance, as well as to identify inter-decade trends.

The first results of these studies were published in the proceedings of the conference [1], where, for the decades 1996-2006 and 2007-2017, the altitude distributions of the seasonal-mean joint ozone-temperature correlation coefficients were presented, as well as a comparison of the seasonal-mean profiles of ozone, temperature and their root-mean-square variations. In this paper, we present expanded and detailed research results and supplement them with a review of more informative distributions of joint ozone-temperature inter-altitude correlation and covariance functions, as well as a comparison of distributions and inter-decade changes in other statistical parameters of ozone and temperature: seasonal-mean structural autocorrelation and autocovariance functions, their frequency spectra, as well as interaltitude correlation and covariance functions.

# 1. Measurement methods and data ensembles

The analysis includes data for the autumn, winter and spring months of 1996-2017 (2096 vertical profiles of the relative content (volume ratio of the mixture) of ozone and the corresponding temperature profiles). Ozone profiles were derieved from brightness temperature spectra of atmospheric thermal radiation at frequencies of the rotational spectral line of ozone  $10_{0,10}$ – $10_{1,9}$  with a central frequency of 142.175 GHz (wavelength 2.1 mm) [15]. The observations were carried out in Moscow at the LPI (55.70° N, 37.57° E, 180 m above sea level). The microwave spectrometer, observation methods, and examples of spectra are discussed in detail in [2, 15, 16].

All the ozone content profiles used in the statistical analysis of this study were obtained from microwave spectra measured during the daytime. The duration of observations was 1-3 hours, the average number of observation days was 15-20 per month (as a rule, all working days, except for days with bad weather) [15,16].

The volume ratio profiles of the ozone mixture were obtained from the measured brightness temperature spectra by solving the corresponding nonlinear integral equation of the 1st kind using an iterative algorithm that was developed in [17] based on the Tikhonov method [18] and described in detail in [2, 19]. This algorithm has been successfully applied in long-term studies of the ozonosphere at the LPI [2,3,19-24].

A detailed analysis of the errors in the retrieval of the ozone profiles performed in these articles, based on numerical simulation using ensembles of profiles, showed that the standard errors of the obtained profiles are very stable and practically independent of variations in ozone profiles and their seasonal statistical ensembles. The errors amount to 0.1-0.2 ppm in a wide range of heights from 15 to 80 km, which is 2-5 % of the average value of the ozone mixture volume ratio in the altitude range of 20-50 km [2]. Considering possible inaccuracies in the temperature and pressure profiles in the kernel of the integral equation being solved, as well as calibration errors and distortions associated with the apparatus function of the spectrometer channels, the actual retrieval error could increase by 1-2 %.

As a result, at altitudes of 20-50 km, the overall error in the retrieval of the ozone profiles did not exceed 5-7 %. Below and above this height range, the errors increased

gradually to 20-30 %. Depending on the specific ozone content profile, measurements are informative in the range from 15-20 to 60-80 km. In this study, we selected an altitude range from 15 to 70 km for statistical analysis. Since 2005, numerous comparisons of the ozone profiles of the LPI have been carried out with those by the MLS Aura instrument [25] over Moscow, which, within the measurement errors of both instruments, showed a coincidence of the ozone profiles for both calm and disturbed states of the stratosphere [23,26].

To retrieve ozone profiles from microwave spectra [27], vertical temperature and pressure profiles were used from the British Atmospheric Data Centre (BADC) database. Meteorological radiosonde data from the Central Aerological Observatory (CAO, Dolgoprudny, Moscow Region) was also sometimes used [28].

In 1996-2009, BADC temperature profiles were available in the altitude range from 0 to 52-66 km; after November 10, 2009, they were available from 0 to 73-80 km. To retrieve the ozone profiles in the mesosphere, the temperature points from BADC were supplemented with a temperature of 191 K at an altitude of 100 km from the CIRA-86 model [29], and then spline interpolation of the temperature profiles was performed. Thus, in the first decade of 1996-2006, there were errors in temperature profiles at altitudes of 60-70 km that could reach 5-10 K or even more due to interpolation errors. During most of the second decade (2007-2017), the BADC temperature profiles at these altitudes were free of these errors. The errors of radiosonde temperature measurements in the altitude range of 0-30 km are less than 1 K [28, 30]. The data presented in [25], based on a comparison between the results from the Aura satellite and other databases, provide estimates of an error of 1 K in the altitude range in the altitude range of 10-80 km and 2.3 K in the range of 80-92 km. In this work, for statistical analysis, we used the same BADC temperature profiles that were previously used to retrieve ozone profiles.

The ensembles of ozone data include 1,169 profiles from the decade 1996-2006 and 927 profiles from the decade 2007-2017. These data have several advantages. Firstly, they were collected in the same location using the same instrument at approximately the same time of day. Secondly, the measurement period covered almost

the entire 23rd and 24th solar activity cycles, which allowed us to analyze long-term changes and their potential correlation with the significant decrease in solar activity during the 24th cycle. For statistical analysis, seasonal ensembles of data were identified, including ozone and temperature profiles for three months of the autumn, winter and spring seasons for each decade. Summer data was not included in the analysis due to minor variations in ozone content.

# 2. Statistical analysis

For the ensembles of ozone and temperature profiles described above, the monthly-mean statistical parameters were calculated by averaging the values for each day of each of the 9 months over 11 years of the decades 1996-2006 and 2007-2017: vertical profiles of the mean ozone volume mixing ratio (content) and mean temperature profile  $\langle T(h) \rangle$ , profiles of their variances:

$$\sigma_U^2(h) = \langle [U(h) - \langle U(h) \rangle]^2 \rangle, \ \sigma_T^2(h) = \langle [T(h) - \langle T(h) \rangle]^2 \rangle$$
 (1)

and the corresponding standard deviations (variations)  $\sigma_U(h)$ ,  $\sigma_T(h)$ , inter-altitude joint ozone-temperature covariance and correlation functions:

$$B_{UT}(h_U, h_T) = \langle [U(h_U) - \langle U(h_U) \rangle] [(T(h_T) - \langle T(h_T) \rangle] \rangle,$$

$$R_{UT}(h_U, h_T) = B_{UT}(h_U, h_T) / \sqrt{B_{UU}(h_U, h_U) B_{TT}(h_T, h_T)},$$
(2)

structure functions (profiles) of ozone and temperature:

$$St_{U}(h,\tau) = \langle [U(h,t) - \langle (U(h,t+\tau) \rangle)^{2} \rangle,$$

$$St_{T}(h,\tau) = \langle [T(h,t) - \langle (T(h,t+\tau) \rangle)^{2} \rangle,$$
(3)

their autocovariance functions:

$$B_{Ut}(h,\tau) = \langle [U(h,t) - \langle U(h) \rangle] [U(h,t+\tau) - \langle U(h) \rangle] \rangle, \tag{4}$$

$$B_{Tt}(h,\tau) = \langle [T(h,t) - \langle T(h) \rangle] [T(h,t+\tau) - \langle T(h) \rangle] \rangle,$$

and autocorrelation functions:

$$R_{Ut}(h,\tau) = B_{Ut}(h,\tau) / \sigma_U^2(h) = B_{Ut}(h,\tau) / B_{UU}(h,h),$$

$$R_{Tt}(h,\tau) = B_{Tt}(h,\tau) / \sigma_T^2(h) = B_{Tt}(h,\tau) / B_{TT}(h,h),$$
(5)

as well as the power spectra of ozone covariance and temperature covariances:

$$S_{U}(h,f) = \int B_{Ut}(h,\tau) \exp(-2\pi i f \tau) d\tau,$$

$$S_{T}(h,f) = \int B_{Tt}(h,\tau) \exp(-2\pi i f \tau) d\tau,$$
(6)

inter-altitude covariance functions of ozone and temperature:

$$B_{UU}(h_1, h_2) = \langle [U(h_1) - \langle U(h_1) \rangle] [U(h_2) - \langle U(h_2) \rangle] \rangle, \tag{7}$$

$$B_{TT}(h_1, h_2) = \langle [T(h_1) - \langle T(h_1) \rangle] [T(h_2) - \langle T(h_2) \rangle] \rangle,$$

and the corresponding correlation functions:

(Fig. 4).

$$R_{UU}(h_1, h_2) = B_{UU}(h_1, h_2) / \sqrt{B_{UU}(h_1, h_1)B_{UU}(h_2, h_2)},$$

$$R_{TT}(h_1, h_2) = B_{TT}(h_1, h_2) / \sqrt{B_{TT}(h_1, h_1)B_{TT}(h_2, h_2)}.$$
(8)

In the above formulas,  $\tau$  is the time shift, and f is the frequency. The seasonal-mean parameters  $X^{ocehb,3llMa,6echa} = \frac{1}{3}\sum_{i=1}^3 X_i$  were obtained by averaging the corresponding monthly average  $X_i$  parameters over the three months of the corresponding season for each of the decades 1996-2006 and 2007-2007. The profiles of the seasonal-mean covariance and correlation coefficients  $B_{UT}(h,h)$ ,  $R_{UT}(h,h)$  are presented in [1]

Estimates show that sampling errors in the monthly-mean variations in ozone and temperature profiles vary relative to the corresponding average profiles from about 7 % in the colder months (November-March) to 17 % in the warmer autumn and spring months. The sample errors in determining the average monthly values of ozone content were in the range of 0.9-1.8 %. In the paper [2], we presented a detailed study of sampling errors in the statistical parameters of the ozone layer profile, including the contribution of errors in the retrieval of the ozone profile from radiometric data. This study showed that errors in the ozone retrieval lead to a relatively small increase in estimates of its standard deviations and covariance functions. Therefore, this factor was not taken into account in their analysis.

The sampling errors of the monthly-mean temperature profiles depend mainly on altitude and range from about 0.3-0.5 K in the troposphere (0.6-0.8 K for September and May) up to 2-3 K in the upper layers. Accordingly, the sample errors of the

seasonal-mean parameters decrease by about 1.7 times. It is important to note that the seasonal instability of ozone and temperature contributes to an increase in their variations and errors in determining average values, especially in the transitional autumn and spring months.

# 3. Results of statistical analysis

Figure 2 shows the ensembles of altitude profiles of ozone and temperature in the stratosphere and lower mesosphere above Moscow, which were used in the analysis, obtained for three seasons of the analysis of two 11-year decades of observations.

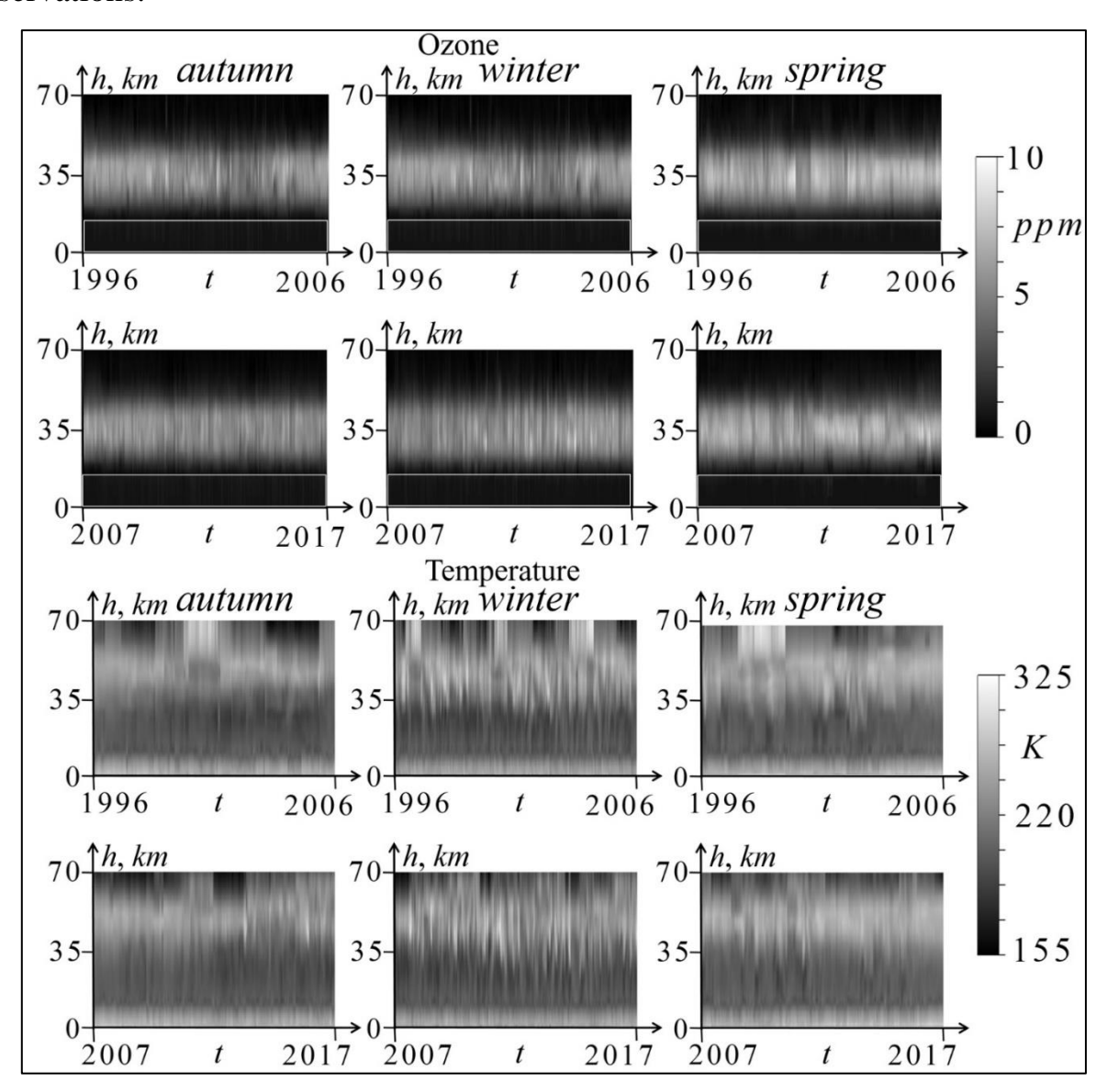


Fig. 2. Ensembles of autumn, winter, and spring ozone and temperature profiles over Moscow in the decades 1996-2006 and 2007-2017. Low-information areas of ozone profiles are highlighted in a white rectangle.

# 3.1. Seasonal-mean profiles and their variations

The corresponding seasonal-mean profiles of ozone content and temperature, as well as the profiles of their root-mean-square variations (1), were presented by us in [1]. Therefore, in this article, Fig. 3 shows only the inter-decade changes (differences) in the seasonal-mean profiles of ozone and temperature, as well as the differences in their variations in a more visual form of diagrams in color gradations. In addition, a much more detailed comparison of these profiles, their variations, and changes in these parameters between the decades 1996-2006 and 2007-2017 is presented below.

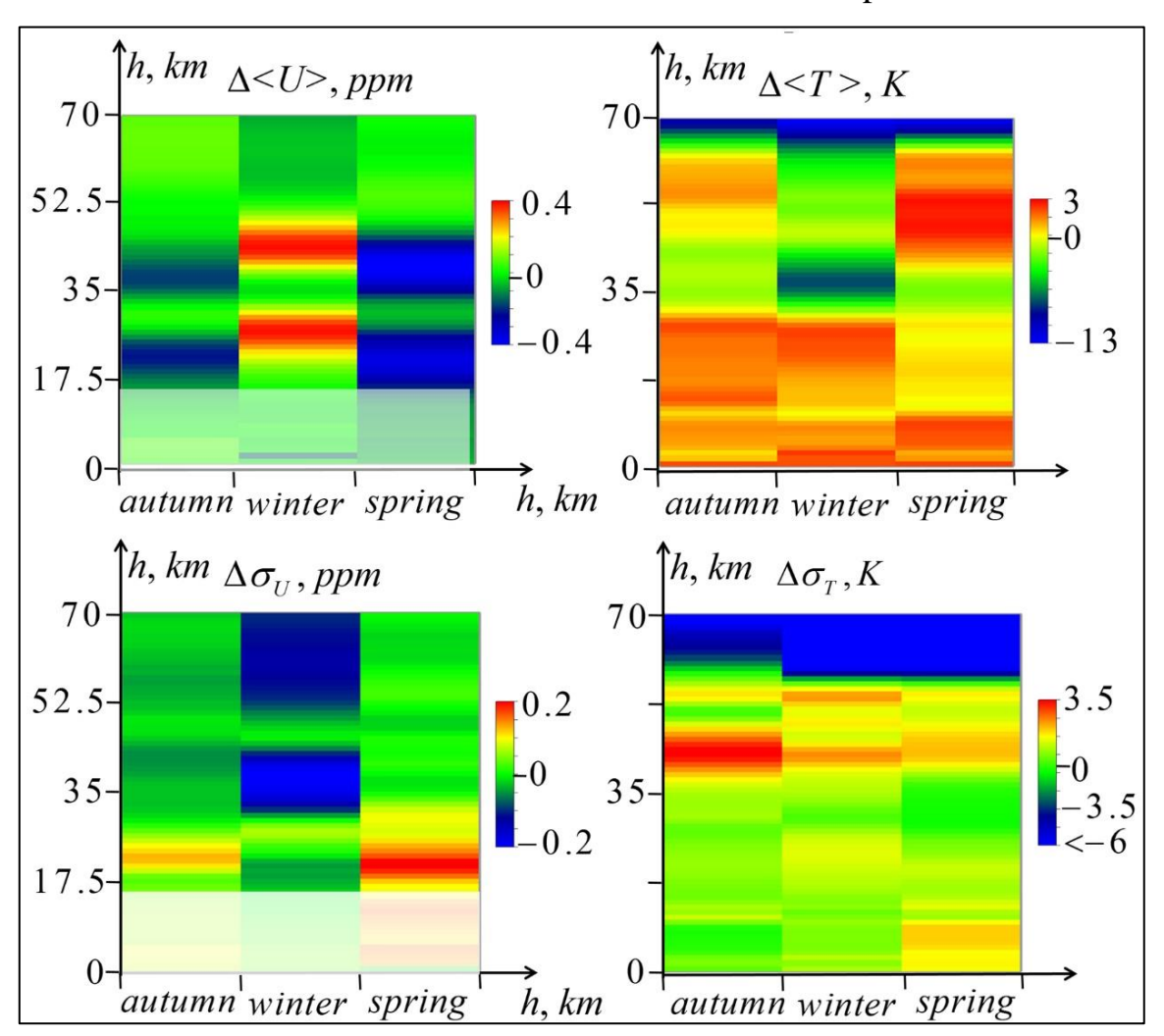


Fig.3. The top row is the inter-decadal (2007-2017 – 1996-2006) change in seasonal-mean profiles of ozone (left) and temperature (right); the lower row is the inter-decadal change in seasonal-mean variations in ozone profiles (left) and temperature (right).

Fig. 3 shows that the inter-decade changes for the winter season differ significantly from the changes in the transitional autumn and spring seasons, which, on the contrary, have many similarities.

In the winter seasonal-mean profiles of ozone content < U > in the decade 2007-2017. (with reduced solar activity), there is an increase in ozone content in layers 15-33 km and 38-52 km with maximum values up to  $\Delta < U > = 0.39$  ppm (about 8 %) at altitudes of 26 and 44 km, respectively, that is, above and below the height of the ozone maximum (about 35 km), where there is a slight decrease of about 0.03 ppm. Conversely, the autumn and spring profiles show a decrease in the average ozone content with two minima of -0.22 and -0.18 ppm (11 and 4 %) at altitudes of 20 and 37 km in autumn and -0.35 and -0.41 ppm (14 and 6 %) at 21 and 40 km in spring. Above 54 km in winter, there is a small (up to 10-15 %) decrease in ozone content, while in autumn and spring there is mostly a slight increase.

Seasonal-mean variations of ozone content  $<\sigma_U>$  in the winter season in the main part of the ozone layer at altitudes of 15-55 km, shown in Fig. 3 in [1], significantly exceed the autumn and spring variations. In the profiles of the average seasonal variations in ozone content, they decreased in the decade 2007-2017 above 29 km in autumn and winter and above 34 km in spring, with a particularly significant drop of  $\Delta\sigma_U=-0.23$  ppm (28 %) in winter at an altitude of 38-39 km, which reflects the decrease in the average monthly values of variations for the winter months found in [2].

In the autumn season, the maximum drop in variations is -0.015 ppm (3 %) at 42 km, and in the spring season it is even less significant. Above 50 km, the differences in winter and autumn variations show second lows: -0.15 ppm at 59 km (39 %) in winter and -0.07 ppm (29 %) at an altitude of 56 km in autumn. At altitudes below 29 km in the winter season, there is an increase in variations in the second decade by 0.05 ppm (5 %) at an altitude of 27 km and a significant (compared with a small average value of variations at this altitude) decrease of -0.07 ppm (47 %) at 20 km. In the autumn and spring seasons at these altitudes, also in the second decade, there is a significant increase in variations with maxima of 0.15 ppm at an altitude of 22 km in

autumn and 0.19 ppm at 20 km in spring, comparable to the average values of variations in the first decade, small at these altitudes.

In the seasonal-mean temperature profiles < T(h) > between 30 and 49 km in the decade of 2007-2017, the most significant decrease in the winter season is observed - to  $\Delta < T(h) > = -8.4$  K at an altitude of 37 km, which overlaps the area of heights of 34-37 km, where there is a decrease in the seasonal-mean ozone profile, located between two areas of its strong increase (see above). This drop in temperature coincides in height with the most significant drop in average winter ozone variations in this decade. Similar correspondences in altitude of the temperature drop maxima (-2.8 K per 42 km in the autumn and -3.2 K per 35 km in the spring) with decrease maxima of the average seasonal-mean ozone content and its variations occur in the autumn and spring seasons. Above 60 km, there is a very significant decrease in temperatures in the second decade, which may contain significant errors related to the interpolation of temperature profiles at these altitudes in the first decade.

There is also a seasonal specificity; an increase in the seasonal-mean temperature in the second decade to  $\Delta < T > = 2.7$  K at altitudes of 41-62 km in spring and a slight (up to 0.7 K) increase by 53-61 km in autumn. Also, in autumn and winter, temperatures rise to 2 K at altitudes from 12 to 30 km. At altitudes of 9-11 km, temperature changes are insignificant, and at altitudes of 2-4 km in autumn and winter, temperatures in the second decade are about 1 K higher, and in spring – by 1.5-2 K. The surface temperature increased in the second decade by 2 K in all three seasons.

Seasonal-mean temperature variations  $<\sigma_T>$  in the winter season in the main part of the ozone layer at altitudes of 15-55 km, shown in Fig. 3 in [1], significantly exceed the autumn and spring variations – as well as the average seasonal variations in ozone mentioned above (Fig. 3 B [1]). In the first decade, they increase from 5 K at an altitude of 15 km to 16.7 K at 38 km (near the maximum of the ozone layer), have a second weak maximum of 15.7 K at 44 km, and decrease to a local minimum of 10.4 K at 54 km. In the second decade, variations increase from 5.1 K at 15 km to 17.9 K at 41 km and decrease to a local minimum of 12.3 K at 55 km. Above 55 km in the first decade, there is a sharp increase in temperature variations to 35 K at 70 km; in the

second decade, this increase continues to a local maximum of 20 K at 67 km (Fig. 3 B [1]). Perhaps, the greater increase in variations with height in the first decade may be due to interpolation errors.

In the winter inter-decadal changes in variations, at altitudes of 15-55 km (see Fig. 3), an increase in temperature variations  $\Delta < \sigma_T >$  is mainly observed: from 0.1 K at an altitude of 15 km to 0.8 K at 23 km. Further, in the altitude range of 28-33 km in the second decade, there is a slight decrease in variations with a minimum value of -0.5 K at 33 km, and above that, there is an increase again, which reaches 1.7 K at 42 km and amounts to 0.8–2 K from 44 to 55 km. It should be noted that in this area of increase in temperature variations, there is a significant decrease in variations in ozone content (see above). Above 55 km, where there is an increase in variations by 2 K in the second decade, a rapid decrease in growth is observed in km, turning into a decrease to -17 K at 70 km, which probably reflects a decrease in the contribution of temperature interpolation errors to variations in this decade.

Referring again to Fig. 3 in [1], it can be seen that temperature variations in autumn and spring are similar. In the first decade, in the 15-55 km layer, they increase from 3.7 K at 15 km to 7.3 K in autumn and 6.1 K in spring, when at an altitude of 36 km there was a local maximum of 8.4 K. Above 55 km, just as in the winter season, there is a sharp increase in temperature variations to 25.7 K at 70 km in autumn and up to 22.8 K in spring, which is significantly lower than in the winter season. In the second decade, the average seasonal variations increase from 3.1 K in autumn and 3.7 K in spring at 15 km to 6.7 K at 51 km with local maxima of 9.1 K at 45 km in autumn and 8.2 K at 40 km in spring. Above 55 km in autumn, temperature variations increase to maxima of 20.3 K at 67 km, and in spring this increase, after a local minimum of 5.5 K at 59 km, reaches 14.2 K at 69 km, which is slightly lower than in the winter season (Fig. 3 B [1]).

From a comparison of the difference in temperature variations  $\Delta < \sigma_T >$  in two decades (see above in Fig. 3), it can be seen that in the autumn season, values close to zero are observed at altitudes of 15-55 km from 15 to 34 km, followed by a layer of elevated values at altitudes up to 48 km with a maximum increase of 3.5 K at 42 km,

followed by a transition to a deep decline at altitudes from 49 to 52 km to a minimum of -0.65 K at 50 km . Further, after a slight increase to 1.2 K at an altitude of 54 km, there is a deep decline to -8.4 K at 70 km.

In the winter season, at altitudes of 15-36 km, there is a slight (up to about 1 K) increase in variations, followed by a slight increase with local maxima of about 2 K at altitudes of 42 and 54 km, followed by a deep decline to -27 K at 70 km.

In the spring season, a small (up to 0.6 K) increase in variations  $\Delta < \sigma_T >$  is observed at altitudes of 15-33 km, followed by a decrease and transition to a decrease in variations at altitudes from 23 to 38 km to about -1 K at altitudes of 30-36 km. Further, in the range of 40-55 km, there is again an increase in the difference in variations with local maxima of 1.7 K at 42 km and 1.2 K at 54 km (at altitudes of similar maxima in the autumn and winter seasons). Above 55 km, there is a rapid decrease in growth, turning into a decline to a local minimum of -8.7 K at 70 km.

In the altitude range of 0-15 km, the profiles of temperature variations  $<\sigma_T>$  have similar distributions in different seasons and decades (see Figs. 3b, 3d, 3f in [1]). In the first decade of the autumn season, there are maximums of the temperature variations of 4.9 K at 0 km, 5.6 K at 6-7 km, 4.7 K at 12 km and lows of 4.6 K at 1 km, 2.8 K at 10 km, 3.3 K at 15 km. In the second decade, at altitudes from 0 to 7 km, variations are almost constant (about 4.5 K), then they decrease to a minimum of 3.4 K at 10 km, rise to a maximum of 5.0 K at 12 km and decrease to 3.4 K at 15 km (Fig. 3 B [1]). In the autumn season, there was a decadal decrease in variations (see above in Fig. 3) at altitudes of 0-9 km with a minimum difference of  $\Delta < \sigma_T > = -1.0$  K at 7 km, its increase to 0.65 K at 10-12 km and a slight decrease to -0.2 K at 15 km.

In the first decade of the winter season, there are maximums of  $<\sigma_T>=6.2$  K at 0 km, 5.8 K at 5 km, 5.7 K per 12 km and lows of 5.0 K at 2 km, 3.1 K at 9 km, 4.9 K at 15 km. In the second decade, there are maxima of 6.5 K at 0 km, 5.7 at 5 km, 5.8 K at 12 km and minima of 5.1 K at 1 km, 3.2 K at 9 km, 5.0 K at 15 km (Fig. 3 B [1]). The inter-decade variations in the winter season did not exceed 0.5 K (see above in Fig. 3).

In the first decade of the spring season, there were maxima of  $<\sigma_T>=4.5$  K at 0 km, 4.6 K at 4-5 km, 4.9 K at 11 km, and minima of 3.2 K at 1 km, 2.6 K at 9 km, 3.4 K at 15 km. In the second decade, there were maxima of 5.6 K at 0 km, 6.1 K at 5 km, 5.7 K at 12 km and minima of 4.3 K at 1-2 km, 3.7 K at 9 km, 3.8 K at 15 km (Fig. 3 B [1]). In the spring season, in the second decade, Fig. 3 (see above) showed an increase in variations from  $\Delta < \sigma_T > = 1.0$  K at 0 km to a maximum of 1.5 K at 5-8 km, a decrease in growth to a minimum of 0.2 K at 10 km, a maximum of 0.9 K at 12 km, and again a decrease in growth to 0.3 K at 15 km.

# 3.2. Ozone-temperature covariance and correlation functions

The studies of seasonal statistical parameters presented at the conference [1] also included altitude distributions of the seasonal-mean ozone-temperature correlation coefficients. In this paper, we consider more informative inter-altitude distributions of joint ozone-temperature covariance and correlation functions (2).

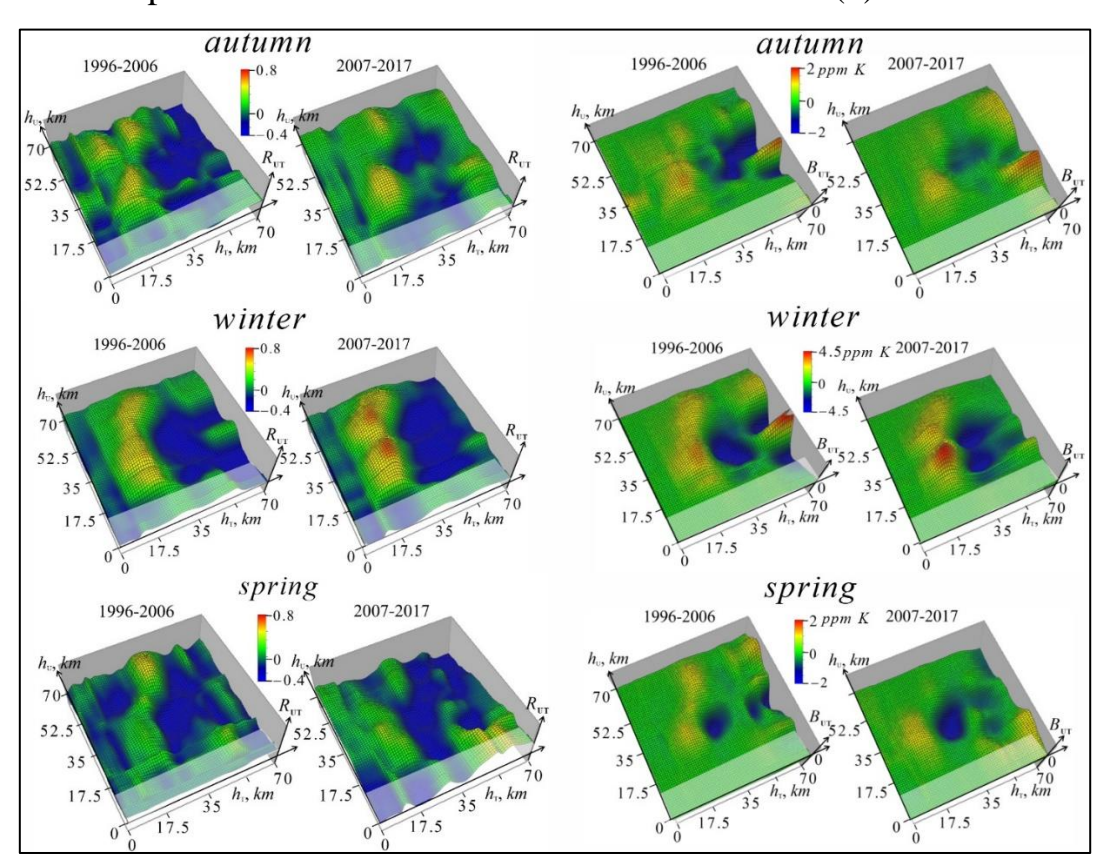


Fig. 4. Seasonal-mean inter—altitude joint ozone-temperature correlation (left) and covariance (right) functions for the decades 1996-2006 and 2007-2017. The top row is the autumn season, the middle row is the winter season, and the bottom row is the spring season.

Fig. 4 shows the seasonal-mean inter-altitude joint ozone-temperature correlation and covariance functions (2) for the decades 1996-2006 and 2007-2017.

As you can see in the figure, the distributions presented have a lot in common — the areas of the greatest correlation of ozone with temperature are observed for temperatures at altitudes below 35 km, and the areas of the greatest anticorrelation are above this altitude. Also, transitions from areas of positive correlation to areas with negative values occur mainly near this height, which is close to the estimates of the heights of transition to anticorrelation and anticovariance in the seasonal-mean profiles of their coefficients presented by us in [1]. However, the heights in the extremes of correlations and anticorrelations in Fig. 4 do not coincide, which demonstrates the greater informational content of two—dimensional correlation functions compared with one-dimensional profiles of correlation coefficients in [1].

A common feature of the distributions in Fig. 4 is the presence of correlation and covariance maxima between the ozone content at altitudes of about 29 km and temperatures at altitudes of about 24 km. Also, in almost all distributions, a second maximum can be seen between ozone at altitudes of about 45 to 60 km and temperatures of about 34 km.

In winter, the correlation maxima turn out to be significantly higher than in autumn and spring; at the same time, they noticeably increase in the decade of 2007-

2017. So, in the autumn season 
$$R_{UT}^{1996-2006}(h_U=38,h_T=23)=0,50$$
,  $R_{UT}^{2007-2017}(h_U=38,h_T=24)=0,52$ , in winter  $R_{UT}^{1996-2006}(h_U=27,h_T=22)=0,60$ ,  $R_{UT}^{2007-2017}(h_U=28,h_T=24)=0,72$ , in spring  $R_{UT}^{1996-2006}(h_U=28,h_T=20)=0,24$ ,  $R_{UT}^{2007-2017}(h_U=30,h_T=15)=0,34$ . The highest secondary correlation maxima are: in autumn  $R_{UT}^{1996-2006}(h_U=48,h_T=19)=0,45$   $R_{UT}^{1996-2006}(h_U=54,h_T=34)=0,49$ , in winter  $R_{UT}^{2007-2017}(h_U=47,h_T=24)=0,70$ , in spring  $R_{UT}^{1996-2006}(h_U=50,h_T=36)=0,52$ .

The areas of anticorrelation are less organized, and their maxima are relatively small: in the autumn season  $R_{UT}^{1996-2006}(h_U=18,h_T=40)=-0,43$ ,  $R_{UT}^{2007-2017}(h_U=43,h_T=51)=-0,48$ , in winter  $R_{UT}^{1996-2006}(h_U=34,h_T=43)=-0,36$ ,

$$R_{UT}^{2007-2017}(h_U = 47, h_T = 45) = -0.48$$
, in spring  $R_{UT}^{1996-2006}(h_U = 34, h_T = 36) = -0.38$ ,  $R_{UT}^{2007-2017}(h_U = 36, h_T = 37) = -0.37$ .

The boundaries between the regions of positive and negative correlation in Fig. 4 coincide with the corresponding boundaries for covariance functions, however, due to the difference in color scales, they look different for these parameters. For correlation functions, crossing the border closely correlates with the transition in the color scale from green to blue, so they are better distinguishable. Due to normalization, the structure of the correlation functions is also clearly detailed in areas with both small and large variations in parameters.

The maxima of covariance and anticovariance in the winter season turned out to be two or more times higher than in autumn and winter:  $B_{UT}^{1996-2006}(h_U=33,h_T=25)=3,4$  ppm K,  $B_{UT}^{1996-2006}(h_U=31,h_T=64)=3,8$  ppm K,  $B_{UT}^{2007-2017}(h_U=28,h_T=25)=4,3$  ppm K,  $B_{UT}^{1996-2006}(h_U=34,h_T=44)=-4,8$  ppm K,  $B_{UT}^{2007-2017}(h_U=44,h_T=45)=-4,3$  ppm K,  $B_{UT}^{2007-2017}(h_U=30,h_T=43)=-3,8$  ppm K.

Below is a comparison of the statistical parameters of ozone and temperature, both within themselves and between their decade-to-decade changes.

## 3.3. Structural functions

Fig. 5 shows the average seasonal structural functions (3) of ozone and temperature variations for the decades 1996-2006 and 2007-2017.

It can be seen that the structural functions of ozone variations reach saturation in 4-7 days. Further, there is some decline, and on the 10-12th day, a secondary maximum can be seen, possibly (especially in the spring season) associated with non-stationarity, or being a manifestation of a periodic process.

The structural functions of temperature in the main region of the ozone layer (15-55 km) are saturated in 3-4 days for the autumn season, in winter – in 10-13 days. In the spring of 1996-2007, saturation occurs in 13 days, and in the decade of 2007-2017, the structural function does not reach saturation, probably due to the non-

stationarity that temperature can manifest itself on any time scale, and especially in such a transitional season as spring.

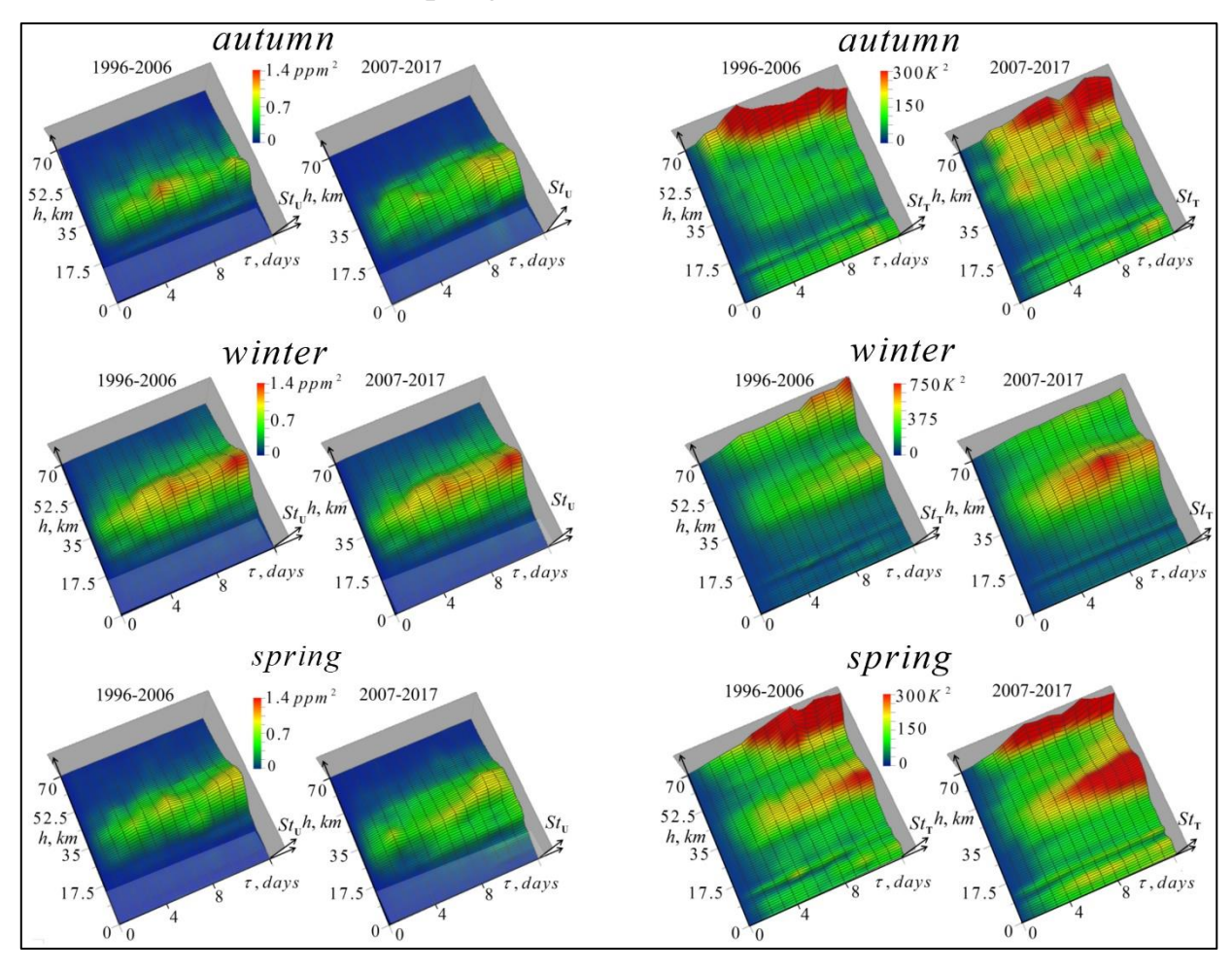


Fig. 5 Seasonal-mean structure functions of ozone (left) and temperature (right) for the decades 1996-2006 and 2007-2017. The top row represents the autumn season, the middle row the winter season, and the bottom row the spring season.

Above 55 km, where the structural functions of temperature are saturated in 3-7 days, non-stationarity does not manifest itself.

# 3.4. Autocovariance functions

Fig. 6 shows the average seasonal autocovariance functions (4) of ozone and temperature variations for the decades 1996-2006 and 2007-2017. The figure shows that in the winter season, the values of the covariance functions of both ozone and temperature are significantly higher than in autumn and spring. At the same time, for the autocovariance functions of ozone in the range of heights of 30-46 km, there is a significant decrease in the decade of 2007-2017 with reduced solar activity (see Fig.1)

compared with the decade of 1996-2006, coinciding with a significant decrease in variations in ozone profiles, and for autocovariance functions of temperature, on the contrary, in the second decade there is a significant increase at no noticeable changes in temperature profile variations.

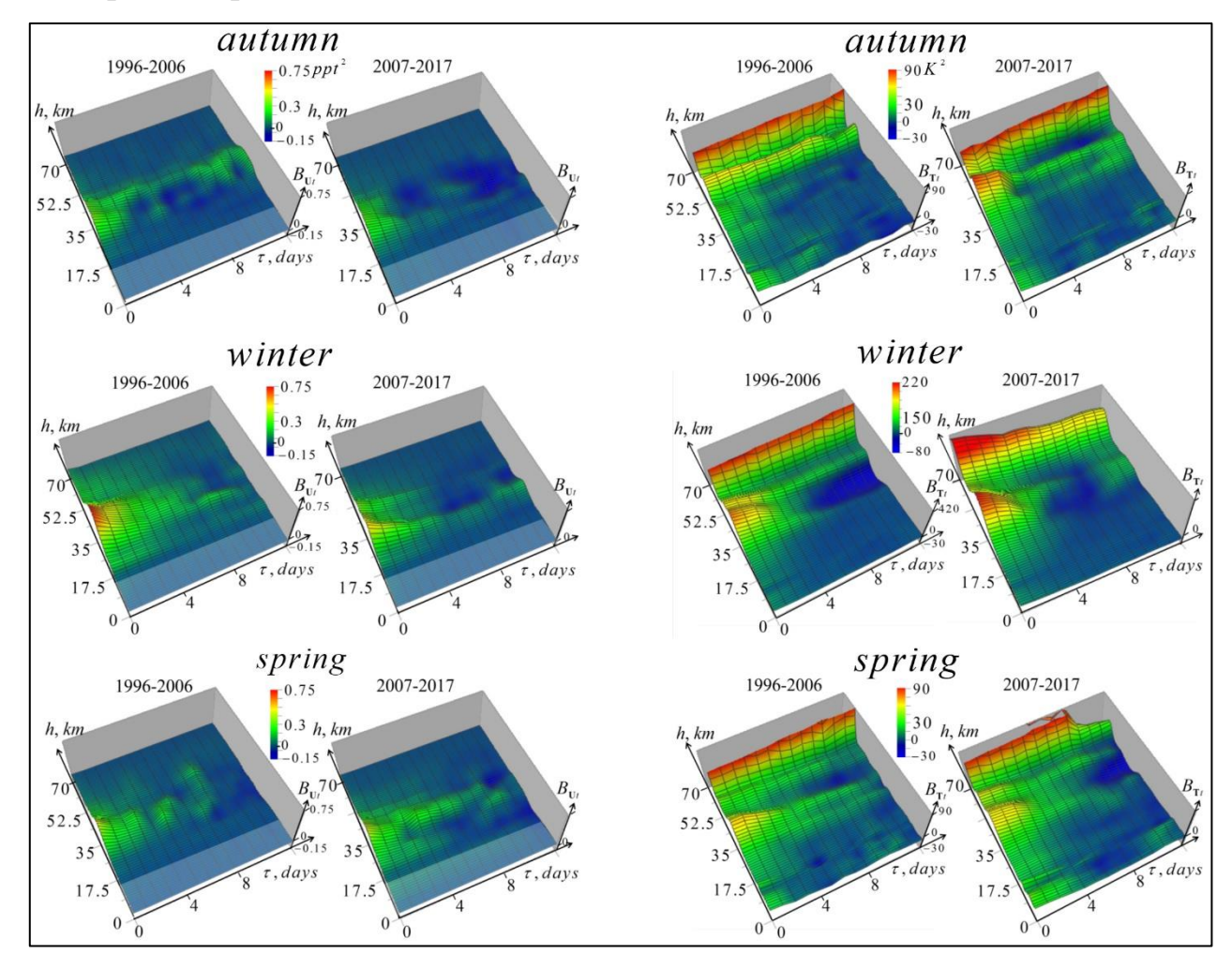


Fig. 6. Seasonal-mean auto-covariance functions of ozone for the decades of 1996–2006 and 2007–2017 (left); corresponding auto-covariances of temperature (right). The top row shows the autumn season, the middle row the winter season and the bottom row the spring season.

The autocovariance functions of ozone decrease with a characteristic time of about 3 days. During this time interval, the highest values of covariances in the autumn season were observed at altitudes of 31-32 km, in winter at 35 km in the decade of 1996-2006 and at 29 km in 2007-2017, and in spring at 32 and 35 km, respectively.

Fig. 6 shows extended layers with small values of ozone covariance, often with local maxima indicating the presence of periodic processes. There are also small areas with negligible negative covariance.

Autocovariance functions of temperature at altitudes of the main part of the ozone layer (15-55 km) also decrease with a characteristic time of about 3 days. During this time interval, in the above-mentioned altitude range, the highest values of temperature covariances in the autumn season were observed at altitudes of 39 km in the decade 1996-2006, and 46 km in 2007-2017, in winter at 38 km and 41 km, and in spring at 36 and 41 km. As can be seen in Fig. 6, the maxima of the highest temperature covariances increased significantly in the second decade.

In the transitional seasons, secondary maxima of temperature covariances are observed at tropospheric heights, indicating periodic meteorological processes. In these seasons, extended layers with small covariance values and secondary maxima can be seen in the stratosphere up to a height of 54 km, reflecting the frequency of processes in the corresponding layers. Above 54 km, there is a sharp increase in covariances with a characteristic attenuation time exceeding the analysis interval shown in Fig. 6.

# 3.5. Autocorrelation functions

Fig. 7 shows the average seasonal autocorrelation functions (5) of ozone and temperature variations for the decades 1996-2006 and 2007-2017.

It can be seen in Fig.7 that the autocorrelation functions of ozone decrease faster in the autumn season than the corresponding autocovariance functions (see Fig. 6), with a typical time of 1-2 days. In the winter season, this time increases to 3-5 days in the first decade and 2-4 days in the second. In the first decade of winter, in the layer up to 35 km, the correlation remains at about 0.2 for the entire analysis interval, and above 55 km – at about 0.1. From 35 to 55 km, the correlation remains at 0.1-0.2 until the 10th-11th day, and then it is replaced by a slight anticorrelation, up to -0.05. In the second decade, this transition occurs on the 8th-9th day, and the anticorrelation in some places reaches -0.1.

In the spring season, the correlation time is from 2 to 5 days. Just as in the autumn correlation functions, there are local maxima of correlation and anticorrelation, indicating various periodic processes.

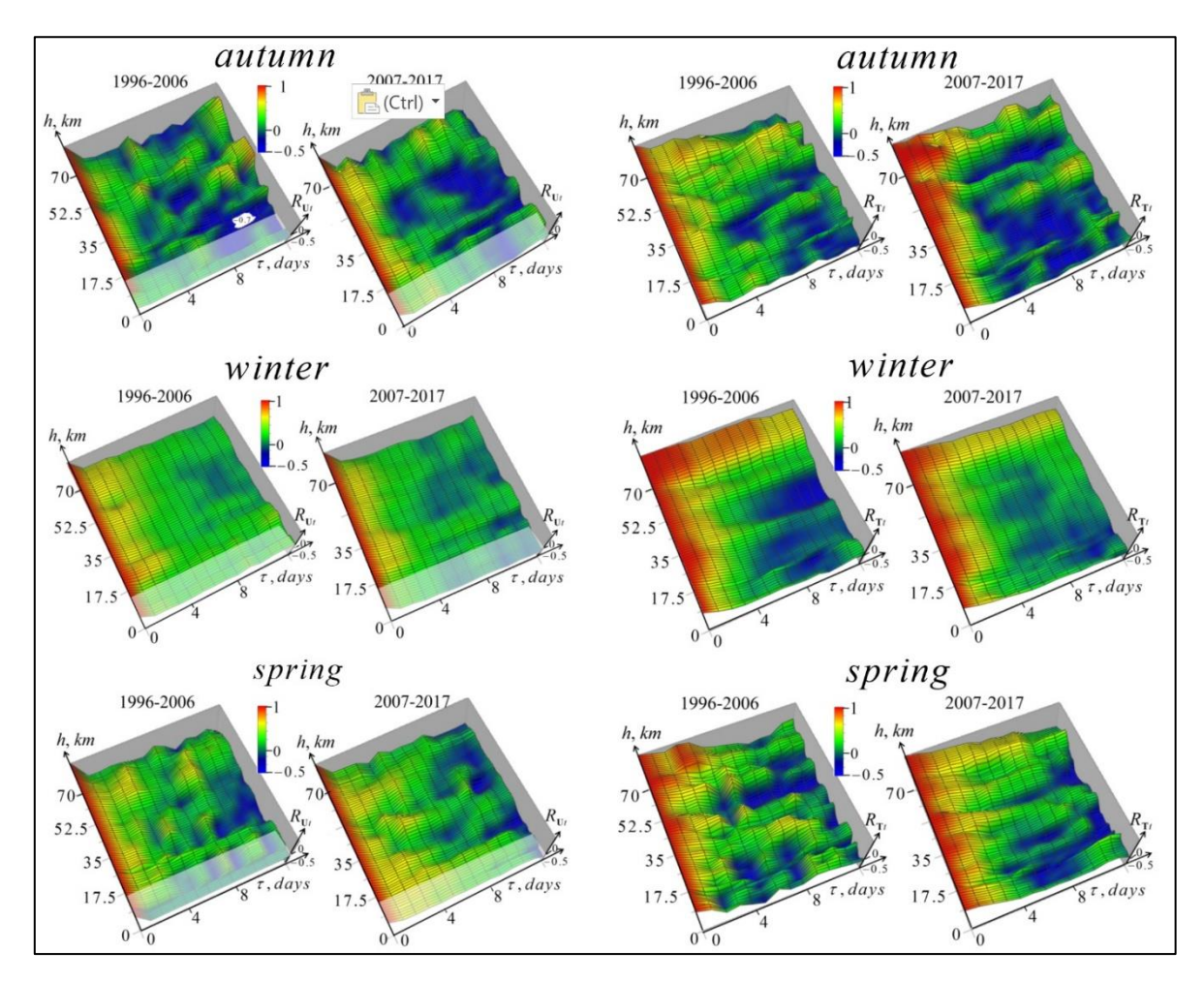


Fig. 7. Seasonal-mean autocorrelation functions of ozone variations for the decades 1996-2006 and 2007-2017 (left); corresponding autocorrelations of temperature variations (right). The top row is for the autumn season, the middle row for winter, and the bottom row for spring.

There are few small areas with anticorrelation extremes R < -0.1 in the autumn season:

$$\begin{split} R_{Ut}^{1996-2006}(h=16,\tau=12) &= -0,71, \ R_{Ut}^{1996-2006}(h=20,\tau=8) = -0,42\,, \\ R_{Ut}^{1996-2006}(h=36,\tau=8) &= -0,40\,, \ R_{Ut}^{1996-2006}(h=49,\tau=12) = -0,30\,, \\ R_{Ut}^{2007-2017}(h=19,\tau=10) &= -0,23\,, \ R_{Ut}^{2007-2017}(h=32,\tau=12) = -0,44\,, \\ R_{Ut}^{2007-2017}(h=43,\tau=5) &= -0,38\,, \ R_{Ut}^{2007-2017}(h=45,\tau=9) = -0,38\,; \\ \text{in spring season} \\ R_{Ut}^{1996-2006}(h=25,\tau=10) &= -0,35 \ \text{and} \ R_{Ut}^{2007-2017}(h=18,\tau=13) = -0,29\,, \\ R_{Ut}^{2007-2017}(h=41,\tau=12) &= -0,48\,, \ R_{Ut}^{2007-2017}(h=51,\tau=13) = -0,24\,. \end{split}$$

There are no areas of significant anticorrelation during the winter season.

# 3.6. Frequency spectra

Fig. 8 shows the frequency spectra (6) of the season-mean autocovariance functions of ozone and temperature for the decades 1996-2006 and 2007-2017.

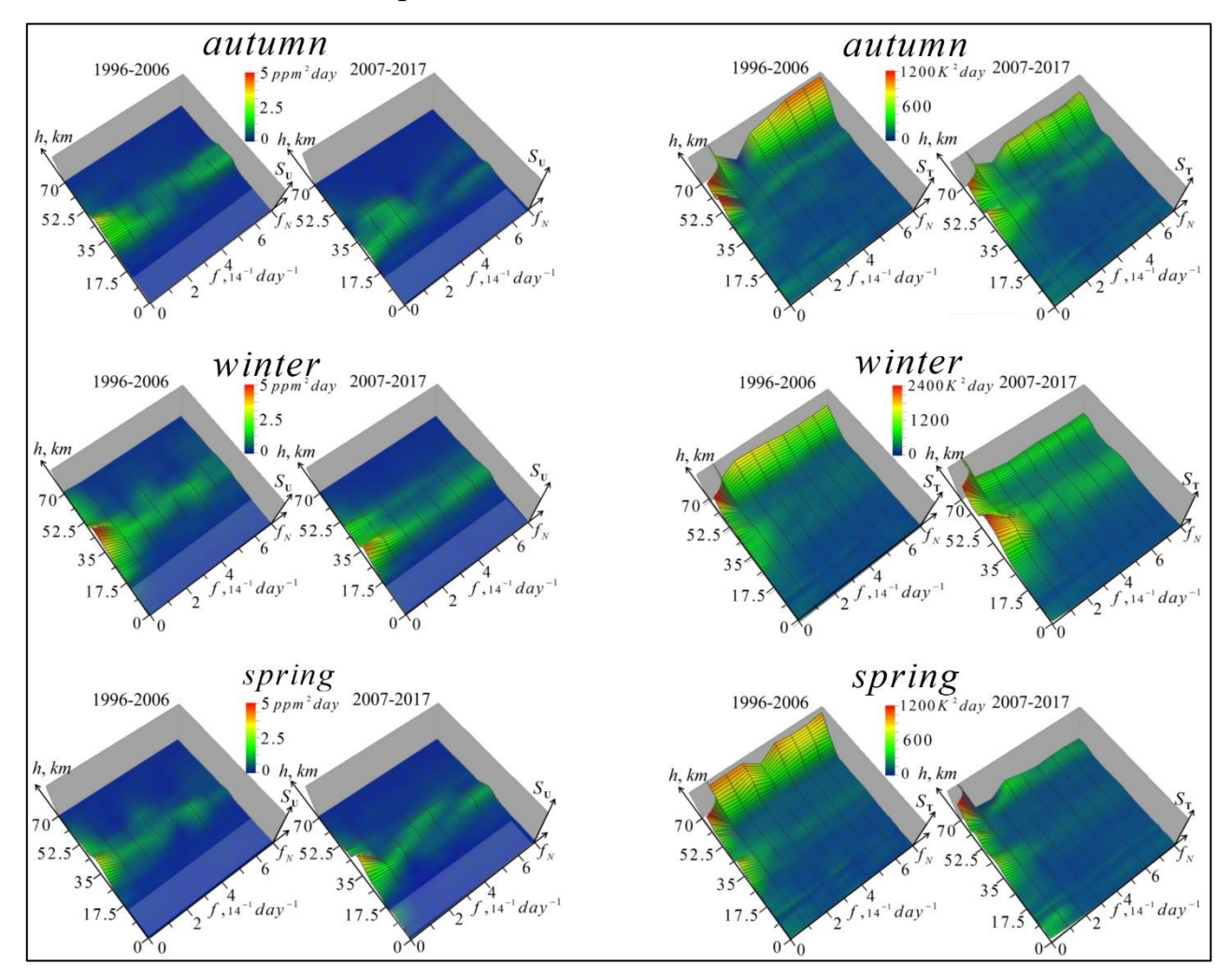


Fig. 8. Frequency spectra of the seasonal-mean autocovariance functions of ozone for the decades 1996-2006 and 2007-2017 (left); corresponding frequency spectra of temperature autocorrelation functions (right). The top row is for the autumn season, the middle row for winter, and the bottom row for spring;  $f_{\rm N=} 0.5 {\rm ~days^{-1}}$  is the Nyquist frequency.

The figure shows that the spectra cover the entire frequency range of the analysis, corresponding to an uneven scale of oscillation periods from 14 to 2 days. In all the spectra, the components corresponding to the period of 14 days are the largest. For both ozone and temperature, the values of the spectra near this period in the second decade were the highest in the winter season. For ozone, the spectrum values for the 14-day component increase slightly in the winter and spring seasons, and decrease in the fall.

The spectral maxima for this component in the first decade are at the following heights: in autumn 33 km, in winter 38 km, in spring 34 km; in the second decade in autumn 28 and 40 km, in winter 30 and 43 km, in spring 29 km.

There are also local spectral ozone maxima with other periods. So, in autumn, in the first decade, we note an increase in the highest frequency 2-3-day spectral components around an altitude of 32 km, in the second decade – about an altitude of 28 km.

In winter, in the first decade, Fig. 8 shows oscillations with a period of about 4 days near the heights of 35 and 46 km and, more strongly, with a period of 2 days, near the height of 35 km. In the second decade, a spectrum extending over the entire frequency range near an altitude of 30 km is clearly visible, with an increase in intensity to the shortest-period components, as well as weaker extended spectra at an altitude of 45 km. In spring, the spectral features of ozone variations in the first decade are close to their position in winter: there are 4-day spectral maxima at altitudes of 46 and 34 km and stronger 2-day maxima at an altitude of 35 km. In the second decade, a 3-4-day maximum at altitudes of about 38 km and a one-day maximum at an altitude of 32 km are most noticeable.

In the frequency spectra of temperature variations, the components corresponding to the period of 14 days are also the largest, and in the winter season of the second decade, the spectrum values near this period increase significantly. Above 60 km, this 14-day maximum is very high and is reached beyond the altitude range shown in the figure. The values of the spectrum of the 14-day component in the 2nd decade also increase slightly in the spring season, and decrease in the autumn. The positions of spectral temperature maxima below 60 km for the 14-day component are as follows: in the first decade in autumn 49, 38, 27, 4 km, in winter 47, 38, 31, 11 km, in spring 35, 11, 4 km; in the second decade in autumn 45 and 11 km, in winter 43, 12, 0 km, in spring 54, 37, 12, 5, 0 km.

In addition, there are local spectral temperature maxima with other periods. In autumn, in the first decade, we note an increase in 3-4-day spectral components around heights of 49 and 36 km, 5-6-day spectral components around 12 km and 3-4-day

spectral components below 6 km in the troposphere, and 1-2-day spectral components near heights of 46 km in the second decade. In winter, in the first decade, there is a noticeable increase in the spectrum in the 2-7-day band at altitudes from 27 to 39 km with a local maximum for 3-4-day fluctuations at 35 km, and in the second decade, there is an extended increase in the spectrum around an altitude of 41 km. In spring, in the first decade, there are 4- and 2-3-day spectral maxima at an altitude of 35 km and 3-4-day ones at about 11 km, and in the second decade, an increase in the spectrum is seen in the range of periods of 2-7 days at altitudes of 33-39 km.

## 3.7. Inter-altitude covariance functions

Fig. 9 shows the seasonal-mean inter-altitude covariance functions (7) for ozone and temperature for the decades 1996-2006 and 2007-2017. One can see some common features in the distributions of the covariance functions of ozone and temperature – an increase in their maximum values in winter, especially significant for temperature functions, and significant changes in the distributions in the second decade.

However, these changes turned out to be in different directions: a sharp drop in covariances for ozone and a sharp increase in covariances for temperature. As expected, the highest covariance values are observed between close altitudes.

The calculated maximum values of the positive covariances turned out to be significantly higher in absolute terms than the negative ones, especially for ozone. It should be noted that, in general, the covariance distributions for ozone and temperature differ greatly from each other. The ozone covariance distributions in Fig. 9 have the following features. The autumn distributions are very similar for the two decades, with a slight decrease in covariances in the second decade.

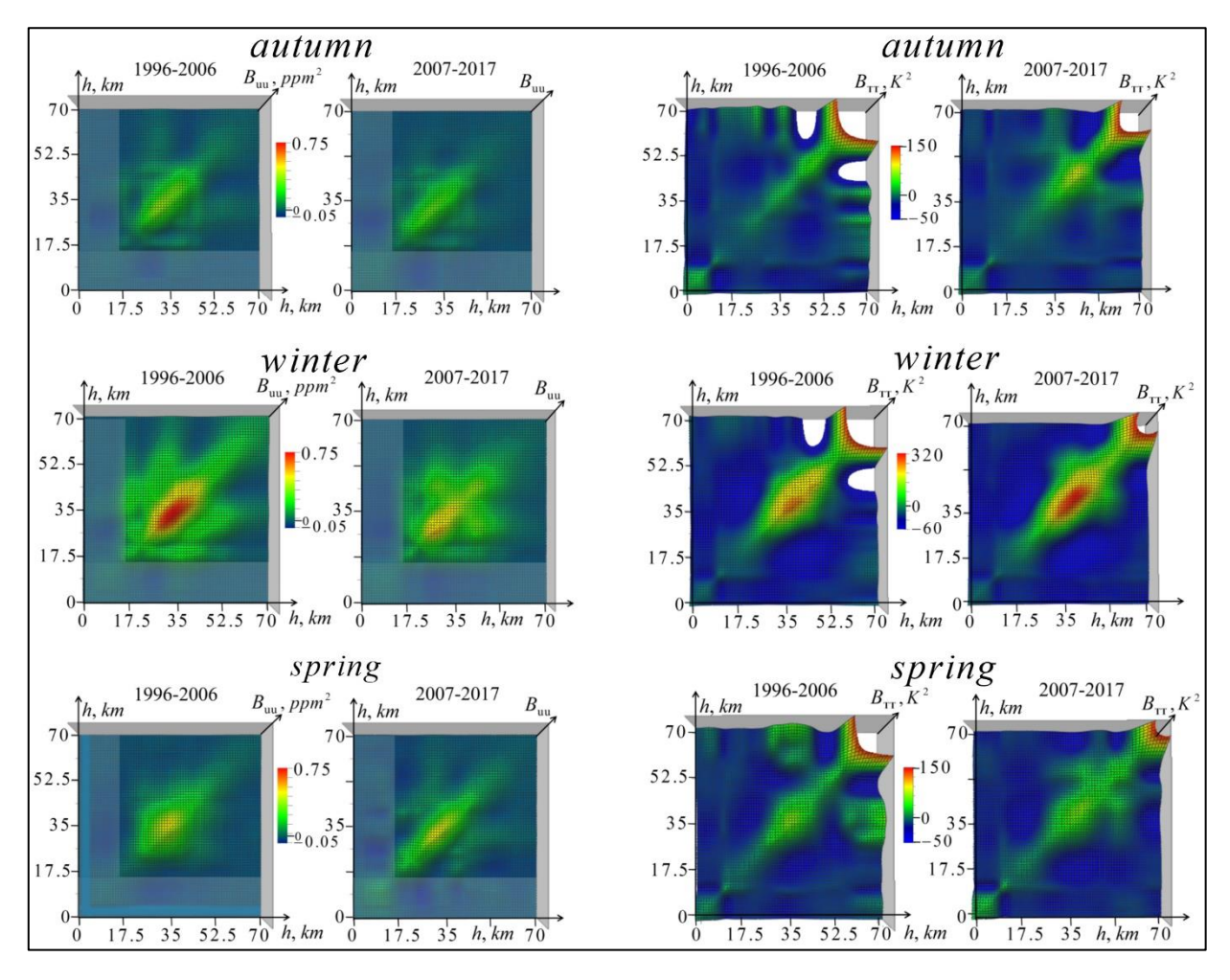


Fig. 9. Seasonal-mean inter-altitude covariance functions of ozone for the decades of 1996–2006 and 2007–2017 (left); corresponding temperature covariance functions (right). The top row shows the autumn season, the middle row shows winter, and the bottom row shows spring.

At a distance from the line of equal heights above the point (15, 15) km, there are two areas of slightly increased covariance and an area of weak negative covariance. In the decade of 1996-2006, increased ozone covariances occur in quadrangular regions with vertex coordinates ( $h_x = 25$  km,  $h_y = 18$  km), (48, 18), (36, 22), (46, 22) km and (45, 24), (69, 24), (52, 37), (70, 37) km, and slightly negative – in the region (54, 39), (70, 39), (60, 45), (70, 47) km. In the decade of 2007-2017, in the areas of increased covariance, there was a slight decrease in its value, while the area of negative covariance narrowed. Coordinates of the vertices of the quadrangular areas of increased positive values: ( $h_x = 30$  km,  $h_y = 17$  km), (49,18), (38, 27), (64, 25) km and (45, 24), (70, 24), (52, 37), (70, 37) km, and of the vertices of the areas of negative values are (51, 35), (54, 35), (53, 39), (54, 39) km.

In the winter season, ozone covariances above 15 km increase significantly compared to autumn and spring and do not contain negative values. At the same time, there is a significant (1.33-fold) decrease in covariances in the 2007-2017 decade, which corresponds to a sharp drop in the corresponding mean square variations in the ozone profile and correlates with a decrease in solar activity in this decade. In winter, the covariance distributions in the two decades are similar in form in basic details, but differ significantly from the autumn and spring distributions. They have maxima on a line of equal heights with values of 0.76 ppm<sup>2</sup> at  $(h_x = 35 \text{ km}, h_y = 35 \text{ km})$  in the first decade and 0.57 ppm<sup>2</sup> at (30, 30) km and 0.33 ppm<sup>2</sup> at (44, 44) km in the second. In both decades, there is a band of weak covariance at an altitude of  $h_v = 20$  km with weakly pronounced maxima with values of 0.20 ppm2 at (39.20) km in the first decade and 0.10 ppm<sup>2</sup> at (46.20) km in the second. Accordingly, at an altitude of  $h_y = 23$  km, there is a linear local minimum in both decades. In the first decade, there is also a wide band of  $h_y$  covariance slowly decreasing along  $h_x = 34$  km. A similar band can be seen in the second decade along the height  $h_x = 31$  km with a local maximum of 0.29 ppm<sup>2</sup> at the point ( $h_x = 47$  km,  $h_y = 31$  km).

The spring covariance functions of ozone at altitudes near the line of equal heights  $h_x = h_y$  exceed the autumn ones, especially in the second decade. According to the maximum values in spring, the inter-decade difference is insignificant, but the distribution of ozone covariances in the second decade is more diverse. In the first decade, the covariance reduction gradients from the line of equal heights are monotonous, and there are no negative covariances. On the contrary, in the decade of 2007-2017, above 15 km, there is a band with local maxima of ozone covariance at coordinates ( $h_x = 41$  km,  $h_y = 20$  km) and (40, 25). There is also a band of elevated values above and below an altitude of 44 km, as well as two regions with weak negative covariances: one inside a rectangle with vertices (47, 15), (70, 15), (54, 25), and (70, 25); the other inside a circle with a radius of 4-5 km and a center at (56, 42).

The distributions of temperature covariances in Fig. 9 differ from ozone covariances by the presence of wide areas of negative values and a sharp increase above 60 km. Below this height, the maxima of temperature covariances on the line of equal

heights are higher than the maxima of ozone covariances on this line, which are near the maxima of the relative ozone content.

In autumn, these temperature covariance maxima are located near the points  $(h_x = 46 \text{ km}, h_y = 46 \text{ km})$  and (49, 49) km in the first and second decades, respectively, in winter at (43, 43) and (42, 42) km, and in spring at (37, 37) km and (41, 41) km.

In the autumn season, in the second decade, there is a 1.33-fold increase in covariance maxima. This increase corresponds to and is obviously due to a significant increase in temperature variations in 2007-2017 (see Fig. 3). Increased covariances with temperatures at altitudes above 55 km are observed for temperatures in the 38-41 km layer in the first decade and 33-41 km in the second. Also, in both decades, there are slightly increased covariances in a narrow layer of 12-14 km with temperatures at altitudes of 12-60 km. Areas of negative temperature covariance values in the first decade include the troposphere relative to temperatures above the tropopause and a rounded area centered at a point ( $h_x = 48 \text{ km}$ ,  $h_y = 24 \text{ km}$ ) that fits into a rectangle. (41, 16), (54, 16), (41, 29), (54, 29) km. In the second decade, negative temperature covariances in the troposphere are observed with respect to temperatures from the tropopause to 55 km. There is also a reduced area of negative covariances with the same center, which fits into the rectangle. (43, 19), (50, 19), (43, 28), (50, 28) km.

In the winter season, below 60 km, there is a more than twofold increase in the maximum values of temperature covariances compared to autumn and spring. This increase reflects an increase in temperature variations (see Fig. 3). There is a 1.15–fold increase in covariance maxima in the second decade compared to the first – less than in autumn (where the increase in temperature variations was greater), but more than in spring. Outside of the covariance values elevated near the line of equal heights in both decades, negative covariances are mainly observed in winter with centers at ( $h_x = 30 \, \text{km}$ ,  $h_y = 6 \, \text{km}$ ) and (44, 22) km in the first decade and (39, 6), (44, 23) km – in the second.

In the spring season, the maximum temperature covariance in both decades is almost the same. On the line of equal heights, there are also secondary maxima near the points (53, 53) km in the first decade and (54, 54) km in the second. In the first

decade, negative temperature covariances of the troposphere are observed with respect to temperatures from the tropopause up to 45 km, and in the second decade – up to 51 km. In each decade, there are two areas of increased negative covariance values with centers at ( $h_x = 39$  km,  $h_y = 22$  km) and (53, 30) km in the first decade and (39, 20), (55, 19) km – in the second. Outside of these regions, the temperature covariance values are weakly negative or weakly positive.

## 3.8. Inter-altitude correlation functions.

Figure 10 shows the seasonal-mean inter-altitude correlation functions (8) for ozone and temperature for the decades 1996-2006 and 2007-2017. As noted above, the boundaries between the regions of positive and negative values of correlation functions coincide with the corresponding boundaries for covariance functions, however, due to the difference in color scales, the position of the boundaries in Figs. 9, 10 may be perceived differently. It can be seen that the structure of the correlation functions of ozone in Fig. 10 is similar to the structure of its covariance functions (Fig. 9), but the areas of these anticovariance boundaries are much more clearly visible in Fig.10.

The same, and even more so, applies to the correlation functions of temperature, since in Fig. 10 it turned out to be possible to demonstrate them at high altitudes, where the corresponding temperature covariance functions (Fig. 9) could not be represented on the selected scale due to their too large values. In the autumn season, Fig. 10 shows that the distribution of strong ozone correlations away from the line of equal heights expands unevenly with increasing altitude, and there are constrictions where correlations decrease faster.

In the decade 1996-2006, such constrictions took place near heights of 15, 20, 25, and 50 km. There is also an extended area of lower correlation. In its trapezoidal part with peaks ( $h_x = 34$  km,  $h_y = 25$  km), (70, 25), (47, 35), (70, 35) km, values of the ozone correlation function are about 0.3. There is a trapezoidal area below (22, 15), (47, 15), (32, 24), (49, 24) km with a local minimum of 0.1 correlation function at (35, 22) km and a maximum of 0.6 at (41, 17) km.

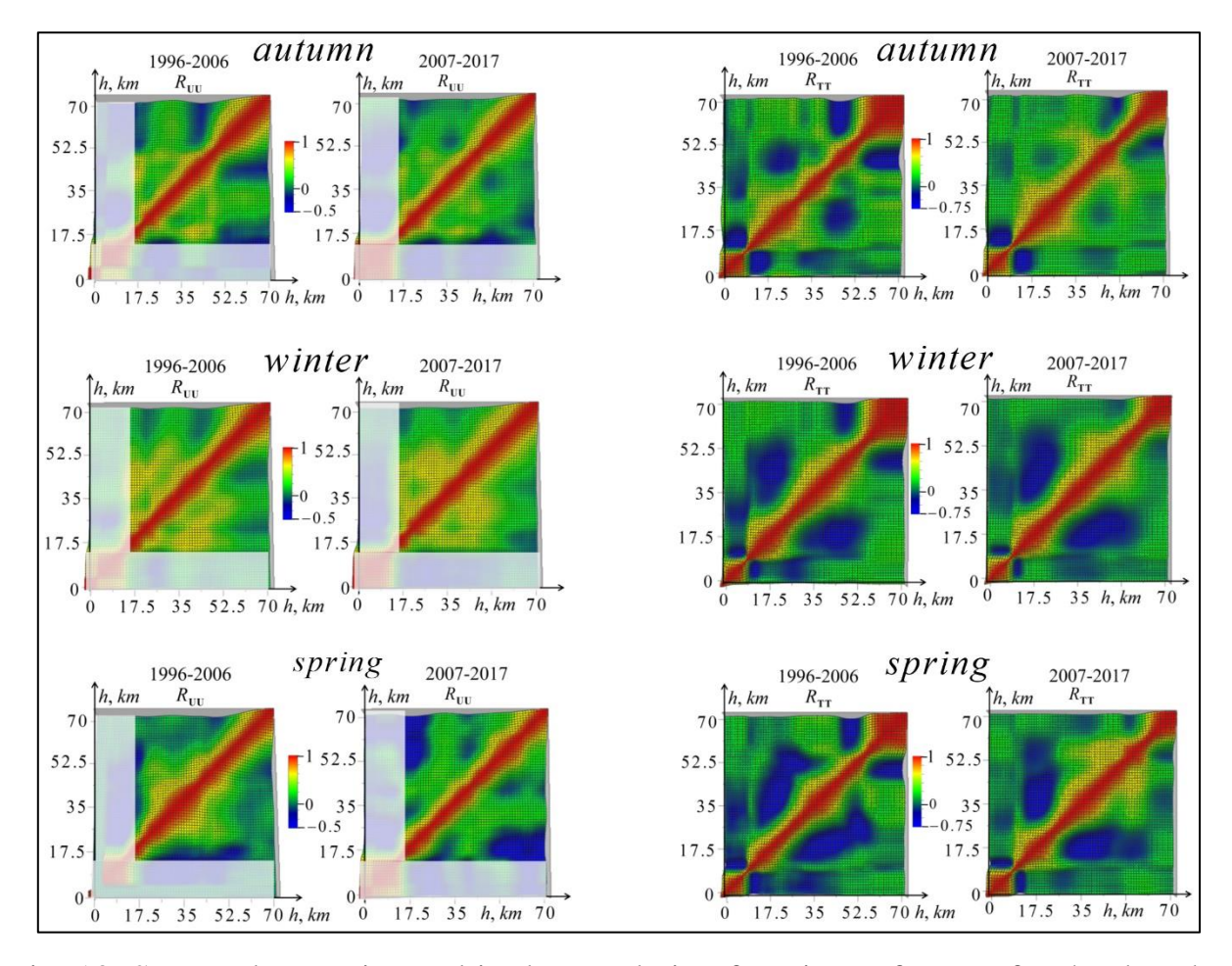


Fig. 10. Seasonal-mean inter-altitude correlation functions of ozone for the decades 1996-2006 and 2007-2017 (left); corresponding temperature correlation functions (right). From top to bottom, the rows represent autumn, winter, and spring seasons.

In addition, there are two areas of small (-0.1...-0.2) km of ozone anticorrelation: (50, 15), (70, 15), (50, 20), (50, 70) km and (53, 40), (70, 40), (53, 41), (70, 47) km.

In the decade of 2007-2017, in the autumn, the area of strong ozone correlation along the line of equal heights also has constrictions near the points ( $h_x = 15$  km,  $h_y = 15$  km) and (20, 20), (25, 25) km, but at an altitude of 50 km, the narrowing is less pronounced. The second trapezoidal region of the first decade is almost preserved: (22, 16), (47, 16), (32, 24), (49, 24) km with a local minimum of 0.15 at (35, 22) km and a maximum of 0.6 at (40, 18) km. The first area with values of the ozone correlation function of about 0.3 is reduced to a triangular area with angles at points: (36, 25), (47, 25), (47, 37) km. Rounded local minima also appeared with a slight anticorrelation of -0.05 at (52.37) km and -0.16 at (69.21) km. There is a slight positive correlation in the rest of the analysis area.

In the winter season, the distribution of strong ozone correlations along the line of equal heights expands unevenly with increasing altitude, alternating with constrictions. In the decade of 1996-2006, as well as in the autumn season, one can see constrictions near the maxima (15, 15), (20, 20), (25, 25) and (50, 50) km. There are no areas of anticorrelation. The pure green borders include an area with correlation values greater than 0.3. There is also an oval area highlighted in yellow with correlation function values greater than 0.5, similar but wider than in autumn, with a maximum of 0.6 at the same point (41, 17) km. Another local maximum is located near the point (45, 25) km.

In the decade of 2007-2017, in winter, one can also see narrowing areas of strong ozone correlations near points of equal heights. (15, 15), (20, 20), (25, 25) However, there is no narrowing around (50, 50) km. The areas of anticorrelation are also missing. From an altitude of 37 km on the line of equal heights (near the ozone maximum) the area highlighted in bright yellow with increased values of the correlation function departs, the boundary of which passes through the points at the 0.6 level ( $h_x = 38$  km,  $h_y = 30$  km), (42, 25), (48, 30) km. Above 37 km on the line of equal heights, the area of increased values of the correlation function gradually expands.

In the spring season, the distribution of strong ozone correlations of ozone along the line of equal heights is less uniform than in autumn and winter. In the decade 1996-2006, it is also possible to see constrictions near the heights of ( $h_x = 15$  km,  $h_y = 15$  km) and (20, 20) km. A specific feature of the distribution of the area of strong ozone correlations along the line of equal heights is its significant broadening at altitudes close to the maximum relative ozone content, away from the point (35, 35) km, amounting to 8 km with a decrease to the correlation level of 0.6. The boundaries of pure green include an area with correlation values greater than 0.3. There are two areas of anticorrelation above  $h_y = 15$  km, colored in blue, with minimum values up to -0.2.

In the decade of 2007-2017, in the spring, one can see a narrowing of the area of strong ozone correlations near the line of equal heights at the points (15, 15), (42, 42) and (60, 60) km. The area with correlation values greater than 0.3 is highlighted in pure green. There is an anticorrelation area inside the rectangle (48, 15), (70, 15), (48, 26),

(70, 26) km with the highest anticorrelation -0.4 at points (55, 18) and (70, 16) km, highlighted in blue, and local minima with low anticorrelation of -0.1 at points (56, 41) and (70, 40) km.

The correlation functions of temperature in the two decades are similar in general structure. In particular, their distributions show wide areas of anticorrelation with deep minima, which predominantly correlate with areas of positive ozone correlation. It should also be noted that since temperature profiles above 60 km were obtained by interpolation in the 1996-2006 decade, this could manifest itself in the greater broadening of the area of strong correlations at these altitudes observed in this decade compared to the 2007-2017 decade.

In the troposphere, one can see a sharp transformation of the temperature correlation functions near an altitude of 10 km, including a sharp contraction at this altitude of the area of increased correlation values along the line of equal heights. At the upper boundary of the troposphere, about 12 km in all seasons and both decades, a thin layer with a near-zero correlation with temperatures above and below this altitude is observed. Also, in all distributions in Fig. 10, there is a significant correlation between temperatures at altitudes in the layer from 0 to 11 km, decreasing from 1 on the line of equal heights to a minimum value  $R_{TT}(h_x = 11 \text{ km}, h_y = 1 \text{ km}) = 0.6$ . In the distributions of the correlation function of tropospheric temperatures in the 0-11 km layer with stratospheric temperatures above 12 km, an area of significant anticorrelation is observed at altitudes from 13 to 18-20 km. The minimum values in this area in autumn are reached at (15, 8) km and amount to -0.76 in the first decade and -0.68 in the second. In winter, the depth of these minima decreases and amounts to -0.57 at (13.8) km and -0.46 at (13.7) km, and in spring -0.60 at (13.8) km in both decades. Correlations of tropospheric temperatures with stratospheric temperatures above 18-20 km are mostly slightly negative, and reach minimum values of -0.4...-0.3 for the seasons under consideration in the first decade. Areas of slight positive correlation with temperatures above 50 km are observed in the corresponding correlation distributions for the second decade.

In the stratosphere and lower mesosphere, in the autumn season of the first decade, in the area of increased correlation values around the line of equal heights, compressions near heights are visible (10, 10), (31, 31), (43, 43) and (54.54) km with subsequent extensions. The areas of a small (0.1-0.3) positive temperature correlation in Fig. 10 are colored green. There are also areas of anticorrelation colored in blue: a rounded area with an anticorrelation value of -0.4 at the central point of (45, 23) km and an area inside the quadrilateral with vertices (55, 43), (60, 51), (70, 43) and (70, 51) km with anticorrelation values of -0.4...-0.65, as well as two small blue-green areas with anticorrelation up to -0.15.

In the second decade of autumn, the area of increased temperature correlation values around the line of equal heights also has a compression of about 10 km and a significant expansion, up to 9 km at the R = 0.6 level, away from the point (24, 24) km. Further, compression to the point (31, 31) km is visible, then up to an altitude of (43,43) km, the width of the zone of increased correlations remains constant, but larger than in the first decade (6 km) Above (43, 43) km, it expands to 9 km, followed by a narrowing to the point (53, 53) km, and starting from the level of (60, 60) km, there is a sharp expansion. The areas of a small (0.1-0.3) positive temperature correlation are colored green. Just as in the first decade, there is a rounded anticorrelation area, but insignificant in magnitude, up to -0.2 at the central point ( $h_x = 45$  km,  $h_y = 23$  km). There is also a region of anticorrelation similar to the first decade in a quadrilateral with vertices. (55, 46), (64, 54), (70, 46), (70, 54) km, but with lower values of -0.2...-0.4, and small blue-green areas with low anticorrelation up to -0.1.

In the winter season, the distributions of the correlation functions of the temperature of the stratosphere and the lower mesosphere differ significantly from the autumn and spring ones: outside the area of high (from 1 to 0.3) correlation, anticorrelation is mainly observed near the line of equal heights. In the first decade of winter, we note the expansion of the zone of correlation values exceeding 0.3: up to 14 km near the point ( $h_x = 12$  km,  $h_y = 12$  km) on the line of equal heights and up to 13-14 km at points of equal heights from (32, 32) to (43, 43) km. An even more significant expansion (but, as noted earlier, overestimated in this decade due to the contribution of

interpolation errors) is observed above the point (55, 55) km. Areas of greatest anticorrelation with values up to -0.35 at (28.5) km in the troposphere, up to -0.5 at (43.18) km in the lower stratosphere, and up to -0.45 at (69.47) km in the upper stratosphere inside a quadrangle with vertices (58, 42), (58, 52), (70, 42), (70, 52) km is represented in blue. The area of a small positive correlation, up to 0.16, is located in a quadrilateral with vertices (54, 0), (60, 21), (70, 0) and (70, 21) km.

In the winter season of the second decade, there are also extensions of the zone of correlation values exceeding 0.3: up to 12 km near the point of equal heights (12, 12) km, up to 13-17 km near the points from (35, 35) to (45, 45) km. Further, a significant expansion of this zone above the (55, 55) km point can also be somewhat overestimated due to the contribution of interpolation errors. The areas of the greatest temperature anticorrelation with values up to -0.2 at the point (35.4) km in the troposphere, up to R = -0.5 at the point of the lower stratosphere (40, 18) km and up to -0.25 at the point (69.51) km in the upper stratosphere inside the quadrangle with vertices (58, 42), (58, 52), (70, 42), (70, 52) km is also represented in blue. In a quadrilateral with vertices ( $h_x = 61$  km,  $h_x = 9$  km), (64, 16), (70, 9) and (70, 16) km is an area of small, up to 0.16, positive correlation.

In the spring season, the areas of temperature anticorrelation turned out to be wider than in the autumn, but narrower than in the winter. In the first decade, there were extensions of the zone of correlation values exceeding 0.6: up to 7 km away from the point (13, 13) km on the line of equal heights, and up to 9 km at altitudes from the point (32, 32) km. An even more significant expansion at altitudes greater than (57, 57) km, as noted earlier, is overestimated. The areas of greatest temperature anticorrelation with values up to -0.57 near the point (11.7) km in the troposphere, up to -0.5 around the point (43.21) km in the lower stratosphere and up to -0.42 at the point (69.50) km in the upper stratosphere within the quadrangle with vertices (57, 46), (61, 53), (70, 46) and (70, 53) km are shown in blue. A positive temperature correlation from 0.15 to 0.4 is observed in a rounded green area centered at (50, 50) km. The areas of correlation with values up to 0.15 are highlighted in a darker shade of green.

In the spring season of the second decade, after the expansion of the zone of temperature correlation values exceeding 0.6 to 8 km, near the point (14, 14) km on the line of equal heights, the width of this zone decreases to 4 km and, starting from the point (33, 33) km, it again expands to 9 km. Further, after some narrowing to 7 km, a local expansion to 13 km is visible at an altitude of (41, 41) km, again narrowing to 5 km near the point (49, 49) km, then widening to 7 km near the point (51, 51) km and then narrowing to 3-4 km from the point (58, 58) km. The subsequent significant expansion of the area of high correlation above (60, 60) km is probably somewhat overestimated. A positive correlation from 0.15 to 0.5 is observed in the green area adjacent to the zone of high temperature correlation values around the line of equal heights. A darker shade of green highlights areas with a lower positive correlation, up to values of 0.15.

# **Conclusion**

The analysis revealed significant differences between the statistical parameters and their inter-decade changes for the winter season from the corresponding characteristics of the transitional autumn and spring seasons, between which, on the contrary, there are many similarities.

A comparison of the seasonal-mean profiles of the relative ozone content and temperature above Moscow, their standard deviations (variations) and the decadal changes in these parameters allowed us to establish that in the winter season in the decade of 2007-2017 with reduced solar activity, the most significant decrease in the seasonal-mean temperature profiles was observed in the layer between 30 and 49 km to -8.4 K at an altitude of 37 km.

This result is particularly interesting because this decrease in the decade with reduced solar activity correlates with the most significant decrease in the average winter variations in ozone above 29 km with a maximum value of -0.23 ppm (28 %) at 38-39 km, as well as with the decrease in the average decadal variations of ozone content, which we discovered earlier [2]. In addition, in the area of this temperature drop, there is an increase in seasonal average temperature variations. There is also a

decrease in the average winter ozone profile at altitudes of 34-37 km between two areas of increasing ozone content in layers of 15-33 km and 38-52 km. Finally, it was found that similar altitudinal correlations of the maxima of temperature decrease with the maxima of decrease in the average seasonal ozone content and its variations occur in the autumn and spring seasons.

It was found that in the winter season, in the main part of the ozone layer at altitudes of 15-55 km, the average seasonal variations in both ozone and temperature significantly exceed the autumn and spring variations.

Among other detected inter-decade changes, it should be noted that in the autumn and spring seasons of the 2007-2017 decade, there was an increase in ozone content variations at altitudes below 29 km with peaks of 0.15 ppm at 22 km in autumn and 0.19 ppm at 20 km in spring, comparable to the average values of variations in the first decade, small at these altitudes.

The average seasonal inter-altitude joint ozone-temperature correlation and covariance functions for the decades 1996-2006 and 2007-2017 were calculated. It was found that the regions of the greatest correlation and covariance of ozone with temperature are observed for temperatures at altitudes below 35 km, and the regions of the greatest anticorrelation and anticovariance are above this altitude. A feature of the distributions is the presence of maxima of correlation and covariance between the ozone content at altitudes of about 29 km and temperatures at altitudes of about 24 km. It is also possible to observe a second maximum correlation between ozone at different altitudes from about 45 to 60 km and temperatures around 34 km.

For the first time, seasonal-mean inter-altitude joint ozone-temperature correlation and covariance functions were applied and obtained in studies of the ozonosphere for the decades 1996-2006 and 2007-2017. It was found that the regions of the greatest correlation and covariance of ozone with temperature are observed for temperatures at altitudes below 35 km, and the regions of the greatest anticorrelation and anticovariance are above this altitude. A common feature of the distributions is the presence of maxima of correlation and covariance between the ozone content at altitudes of about 29 km and temperatures at altitudes of about 24 km. It is also possible

to observe a second maximum correlation between ozone at different altitudes from about 45 to 60 km and temperatures around 34 km. The exact positions and values of the extremes of correlation and anticorrelation are given, as well as the positions of the boundaries of the corresponding regions. The areas of anticorrelation are less ordered, and its maxima are relatively small. In winter, the correlations turn out to be significantly higher than in autumn and spring; at the same time, they increase markedly in the decade of 2007-2017.

The new information was obtained by comparing the distributions and trends of the seasonal-mean structural, autocovariance, and autocorrelation functions of ozone and temperature variations, as well as their frequency spectra.

It turned out that the structural functions of ozone covariations reach saturation in 4-7 days. There is also a secondary maximum, possibly related to non-stationarity or being a manifestation of a periodic process. The structural functions of temperature in the main region of the ozone layer (15-55 km) are saturated in 3-4 days for the autumn season, in winter – in 10-13 days. In the spring of 1996-2006, saturation occurred in 13 days, and in the decade of 2007-2017, the structural function did not reach saturation.

A study of the seasonal-nean autocovariance functions of ozone and temperature variations showed that their values were significantly higher in the winter season than in autumn and spring. At the same time, for ozone functions in the range of maxima of 30-46 km, there was a significant decrease in the decade of 2007-2017 with reduced solar activity compared to the decade of 1996-2006, coinciding with a significant decrease in the standard deviations of ozone profiles. On the contrary, the temperature functions showed a significant increase in the absence of noticeable changes in variations. The autocovariance functions of ozone decrease with a characteristic time of about 3 days, and the presence of local maxima in them indicates the presence of periodic processes.

The autocovariance functions of temperature at altitudes of 15-55 km also decrease with a characteristic time of about 3 days; at the same time, the maxima of the greatest temperature covariances increased significantly in the second decade.

Secondary maxima are visible in the troposphere during the transitional seasons (autumn and spring), indicating periodic meteorological processes. In these seasons, extended layers with small covariance values and secondary maxima reflecting periods of processes in the corresponding layers were noticeable in the stratosphere up to an altitude of 54 km. Above 54 km, there is a sharp increase in temperature covariances with a characteristic attenuation time exceeding the analysis interval.

The autocorrelation functions of ozone decrease in the autumn season with a characteristic time of 1-2 days. In the winter season, this time is up to 3-5 days in the first decade and up to 2-4 days in the second. In the spring season, the correlation time is from 2 to 5 days. Just as in the autumn correlation functions, in spring there are local maxima of ozone correlation and anticorrelation, indicating various periodic processes.

The results of the analysis of the frequency spectra of the average seasonal autocovariance functions of ozone and temperature showed that these spectra cover the entire frequency range of the analysis, and the spectral components corresponding to the period of 14 days are the largest. For both ozone and temperature, the spectral values near this period in the second decade are significantly higher in the winter season. The spectral maxima for the 14-day component in the first decade are at altitudes: 33 km in autumn, 38 km in winter, 34 km in spring; in the second decade: 28 and 40 km in autumn, 30 and 43 km in winter, 29 km in spring. Other local spectral maxima correspond to periods of ozone fluctuations of 1-4 days.

In the temperature frequency spectra, the components corresponding to the period of 14 days in the decade of 2007-2017 increase significantly in the winter season, and also increase slightly in spring, and decrease in autumn. Above 60 km, this 14-day maximum is very high. The positions of the observed spectral maxima below 60 km for the 14-day component in the first decade: autumn 49, 38, 27, 4 km, winter 47, 38, 31, 11 km, spring 35, 11, 4 km; in the second decade: autumn 45 and 11 km, winter 43, 12, 0 km, in spring 54, 37, 12, 5, 0 km. Other local spectral temperature maxima have periods of 1-7 days.

A detailed study and comparison of the average seasonal inter-altitude covariance and correlation functions for ozone and temperature for the decades 1996-2006 and 2007-2017 was also performed.

Common features were identified in the distributions of ozone and temperature covariance functions: an increase in their maximum values in winter, especially significant for temperature functions, and significant changes in distributions in the decade of 2007-2017. But these changes turned out to be multidirectional: a sharp drop in ozone covariances and a sharp increase in temperature. The highest covariance values are observed between close altitudes. The maximum absolute values of the positive covariances were significantly higher than the negative ones, especially for ozone. The details of the structure of the distributions of covariance functions are described in detail.

The autumn distributions of ozone covariances are similar for the two decades, with a slight decrease in covariances in the second decade. The spring covariance functions at heights near the line of equal heights exceed the autumn ones, especially in the second decade. According to the maximum values of covariances in spring, the difference between the decades is insignificant, but the distribution of ozone covariances in the second decade is more diverse. In the first decade, the covariance reduction gradients from the line of equal heights are monotonous, and there are no negative covariances.

In the winter season, ozone covariances above 15 km increase significantly compared to autumn and spring and do not contain negative values. At the same time, there is a significant (up to 1.33 times) decrease in covariances in the 2007-2017 decade, which corresponds to a sharp drop in the corresponding height variations in the ozone profile and correlates with a decrease in solar activity in this decade.

The distributions of temperature covariances differ from ozone covariances in the presence of wide areas of negative values and a sharp increase above 60 km. Below this height, the maxima of temperature covariance on the line of equal heights are located above the maxima in the distributions of ozone covariances on this line, which are near the maximum of the relative ozone content.

In the autumn season of the second decade, the temperature covariance maxima increased by about 1.33 times. This increase corresponds to and is obviously due to a significant increase in the standard deviations (variations) of temperature in autumn in 2007-2017. In the winter season of the second decade, there is a more than twofold increase in the maximum values of covariances compared to autumn and spring. This growth reflects an increase in temperature profile variations. In winter, there was also a 1.15–fold increase in covariance maxima in the second decade compared to the first – less than in autumn, but more than in spring, when covariance maxima in the two decades were almost the same.

The structure of the seasonal average correlation functions of ozone is similar to the structure of its covariance functions, but due to their normalization by one, the details of correlations in areas with small absolute values are more clearly discernible. In autumn and winter, the distribution of strong ozone correlations away from the line of equal heights expands unevenly with increasing altitude, narrowing is observed, where correlations decrease more quickly. There are no areas of anticorrelation during the winter season. In the spring season of the decade 1996-2006, a specific feature of the distribution of the area of strong correlations along the ozone line of equal heights is its significant broadening at altitudes close to the ozone maximum of about 35 km.

The structures of the temperature correlation functions in the two decades are very similar. The distributions of the temperature correlation functions show wider areas of anticorrelation than in the ozone functions, and with deeper minima. As a rule, these areas are located in areas of increased ozone correlation. It is also possible to see a sharp transformation of the temperature correlation functions in the upper troposphere near an altitude of 10 km, including a sharp contraction at this altitude of the area of increased correlation values along the line of equal heights. A detailed description and comparison of the structure of correlation functions for the decades 1996-2006 and 2007-2017 is given.

The authors are grateful to former researchers of the FIAN S.V. Solomonov, scientific director of the Laboratory of Millimeter Wave Spectroscopy of the LPI and

E.P. Kropotkina, as well as A.N. Ignatiev and A.N. Lukin, who helped to obtain data from long–term measurements of ozone profiles used in this work.

**Financing:** This study has been supported by the Ministry of Science and Education of Russian Federation, program FFUF-2024-0019.

## References

- Gaikovich K. P., Rozanov S. B. Ozone and Temperature Seasonal Statistics by Data of 1996-2017 Ground-Based Microwave Radiometry //2024 IEEE 9th All-Russian Microwave Conference (RMC). IEEE, 2024. P. 12-15.
   https://doi.org/10.1109/RMC62880.2024.10846815
- 2. Gaikovich K. P., Kropotkina E. P., Rozanov S. B. Statistical analysis of 1996–2017 ozone profile data obtained by ground-based microwave radiometry //Remote Sensing. 2020. V. 12. No. 20. P. 3374. https://doi.org/10.3390/rs12203374
- Gaikovich K. P., Kropotkina E. P., Rozanov S. B. Statistical parameters of ozone profiles above Moscow and their trends in 1996-2017 by data of radiometer measurements // Zhurnal Radioelektroniki [Journal of Radio Electronics]. 2021.

   No.8. (In Russian) https://doi.org/10.30898/1684-1719.2021.8.14
- 4. Montzka S. A. et al. Scientific assessment of ozone depletion: 2010 //Global Ozone Research and Monitoring Project-Report No. 51. – 2011. https://ozone.unep.org/sites/default/files/2023-02/Scientific-Assessment-of-Ozone-Depletion-2022.pdf
- 5. Moreira L. et al. The natural oscillations in stratospheric ozone observed by the GROMOS microwave radiometer at the NDACC station Bern //Atmospheric Chemistry and Physics. 2016. V. 16. No. 16. P. 10455-10467. https://doi.org/10.5194/acp-16-10455-2016
- 6. Randel W. J. et al. A simple model of ozone–temperature coupling in the tropical lower stratosphere //Atmospheric Chemistry and Physics. 2021. V. 21. No. 24. P. 18531-18542. https://doi.org/10.5194/acp-21-18531-2021

- 7. Brasseur G. P., Solomon S. Aeronomy of the middle atmosphere: Chemistry and physics of the stratosphere and mesosphere. Dordrecht: Springer Netherlands, 2005.
- Stolarski R. S. et al. Ozone temperature correlations in the upper stratosphere as a measure of chlorine content //Journal of Geophysical Research: Atmospheres. 2012. V. 117. No. D10. https://doi.org/10.1029/2012JD017456
- 9. Huang F. T. et al. Ozone quasi-biennial oscillations (QBO), semiannual oscillations (SAO), and correlations with temperature in the mesosphere, lower thermosphere, and stratosphere, based on measurements from SABER on TIMED and MLS on UARS //Journal of Geophysical Research: Space Physics. 2008. V. 113. No. A1. P. A01316. https://doi.org/10.1029/2007JA012634
- 10. Huang F. T. et al. Ozone and temperature decadal trends in the stratosphere, mesosphere and lower thermosphere, based on measurements from SABER on TIMED //Annales geophysicae. Göttingen, Germany: Copernicus Publications, 2014. V. 32. No. 8. P. 935-949. https://doi.org/10.5194/angeo-32-935-2014
- 11. Huang F. T. et al. Ozone and temperature decadal responses to solar variability in the mesosphere and lower thermosphere, based on measurements from SABER on TIMED //Annales Geophysicae. Göttingen, Germany: Copernicus Publications, 2016. V. 34. No. 1. P. 29-40. https://doi.org/10.5194/angeo-34-29-2016
- 12. Huang F. T., Mayr H. G. Ozone and temperature decadal solar-cycle responses, and their relation to diurnal variations in the stratosphere, mesosphere, and lower thermosphere, based on measurements from SABER on TIMED //Annales Geophysicae. Göttingen, Germany: Copernicus Publications, 2019. V. 37. No. 4. P. 471-485. https://doi.org/10.5194/angeo-37-471-2019
- Zhou L., Xia Y., Zhao C. Influence of stratospheric ozone changes on stratospheric temperature trends in recent decades //Remote Sensing. 2022. V. 14. No. 21. P. 5364. https://doi.org/10.3390/rs14215364
- 14. Hocke K., Sauvageat E. Frequency Dependence of the Correlation between Ozone and Temperature Oscillations in the Middle Atmosphere //Atmosphere. 2023. V. 14. No. 9. P. 1436. https://doi.org/10.3390/atmos14091436

- 15. Solomonov S. V. et al. A millimeter-wave spectroradiometer for the remote sensing of atmospheric ozone // J. Commun. Technol. Electron. 2000. V. 45. P. 1377–1382.
- 16. Solomonov S. V. et al. Spectral instrumentation for monitoring atmospheric ozone at millimeter waves // Instrum. Exp. Tech. 2009. V. 52. P. 280–286. https://link.springer.com/article/10.1134/S0020441209020286
- 17. Gaikovich K. P. Tikhonov's method of the ground-based radiometric retrieval of the ozone profile //Proceedings of IGARSS'94-1994 IEEE International Geoscience and Remote Sensing Symposium. IEEE, 1994. V. 4. P. 1901-1903. https://gaikovich.narod.ru/papers/IGARSS94\_1.pdf
- 18. Tikhonov A. N., Arsenin V. Y. Solutions of ill-posed problems. New York: Winston USA, 1977.
- 19. Gaikovich K. P., Kropotkina E. P., Solomonov S. V. Vertical ozone profile determination from ground-based measurements of atmospheric millimeter-wave radiation //Izvestiya Atmospheric and Oceanic Physics. – 1999. – V. 35. – No. 1. – C. 78-86. https://gaikovich.narod.ru/papers/AOPh1\_99.pdf
- 20. Solomonov S. V. et al. Remote sensing of atmospheric ozone at millimeter waves //Radiophysics and Quantum Electronics. 2011. V. 54. No. 2. P. 102-110. https://link.springer.com/article/10.1007/s11141-011-9274-8
- 21. Kropotkina E. P. et al. Characteristics of Changes in the Ozone Content in the Upper Stratosphere over Moscow during the Cold Half-Years of 2014–2015 and 2015–2016 //Geomagnetism and Aeronomy. 2019. V. 59. No. 2. P. 212-220. https://doi.org/10.1134/S0016793219010092
- 22. Solomonov S. V. et al. Some features of the vertical ozone distribution from millimeter wave measurements at Pushchino and Onsala observatories //Journal of atmospheric and terrestrial physics. 1994. V. 56. No. 1. P. 9-15.
- 23. Rozanov S. B. et al. Ground-based remote sensing of the atmospheric ozone over Moscow at millimeter waves //Remote Sensing of Clouds and the Atmosphere XI. SPIE, 2006. T. 6362. C. 464-474.

- 24. Solomonov S. V. et al. Influence of strong sudden stratospheric warmings on ozone in the middle stratosphere according to millimeter wave observations //Geomagnetism and Aeronomy. 2017. T. 57. №. 3. C. 361-368. https://link.springer.com/article/10.1134/S0016793217020141
- 25. Kropotkina E. P. et al. Characteristics of Changes in the Ozone Content in the Upper Stratosphere over Moscow during the Cold Half-Years of 2014–2015 and 2015–2016 //Geomagnetism and Aeronomy. 2019. V. 59. No. 2. P. 212-220. https://doi.org/10.1134/S0016793219010092
- 26. Rozanov S. B. et al. Microwave measurements of stratospheric and mesospheric ozone in Moscow //IGARSS 2018-2018 IEEE International Geoscience and Remote Sensing Symposium. IEEE, 2018. P. 3116-3119. https://doi.org/10.1109/IGARSS.2018.8518910
- 27. The British Atmospheric Data Centre (BADC). http://badc.nerc.ac.uk/view/badc.nerc.ac.uk\_ATOM\_dataent\_ASSIM
- 28. The Central Aerological Observatory, Dolgoprudniy. http://aerology.org
- 29. COSPAR International Reference Atmosphere (CIRA-86). https://www.aparc-climate.org/data-centre/data-access/reference-climatology/cira-86
- 30. Sounding systems and radiosondes // Vaisala. https://www.vaisala.com/en/sounding-systems-radiosondes/

## For citation:

Gaikovich K.P., Rozanov S.B. Comparison and correlations of seasonal-mean statistical parameters of stratospheric ozone and temperature by data of ground-based radiometric and satellite measurements for 1996-2017 // Journal of Radio Electronics. - 2025. - N 10. https://doi.org/10.30898/1684-1719.2025.10.6